Long-Boom Trimming Yagis: An Accumulation of Data

L. B. Cebik, W4RNL
1434 High Mesa Drive
Knoxville, TN 37938
e-mail: cebik@cebik.com

The "trimming" Yagi is actually a Yagi series with some minimum number of elements to some maximum number. The classic design belongs to Gunter Hoch, DL6WU. The operative theory is that to make a Yagi shorter than the maximum number of elements (but larger than the minimum number of elements), one only needs to eliminate the required number of forward directors. The performance of the shorter version will be appropriate to the new boomlength, while the main operating curves for gain and feedpoint impedance will be comparable at any boomlength in the allowable sequence.

The trimming Yagi has received only spot checks, at least so far as the literature at my disposal is concerned. Lacking is a systematic investigation of the performance of the array at every boomlength within some significant set of limits. Such an exploration is well suited to NEC-4 modeling analysis. For example, one might explore some version of the DL6WU series between 10 and 40 elements. At 432 MHz, a 40 element version yields a boom just over 14 λ. I undertook just such an expedition in preparation for exploring in detail the behavior of 2-stacks. However, the increment of boomlength change per new director proved too wide for completely satisfactory results. Therefore, I developed a second series of trimming Yagis using the VK3AUU impedance-setting cell and a progression of directors developed from regression analysis. The resulting Yagis have quite different characteristics from the VK3AUU original design, since the goal was to draw the design closer to the DL6WU series. The key factor in the design is the use of more closely spaced elements so that a 50-element test-seriesYagi design is only a small bit longer than a 40-element DL6WU design.

The results are 31 DL6WU Yagi models and 41 test-Yagi models, each one frequency swept from 400 to 460 MHz. Within that span is the 70-cm amateur band from 420 to 450 MHz. The design frequency is 432 MHz. The data accumulated from the models is worth exploring for several reasons. First, there are a number of intriguing patterns both within each Yagi series and when we compare the series. Second, there are a number of design and operating equations floating about in long-boom Yagi lore that deserve comparison to the modeled data. Third, there are a number of design considerations, hitherto passed over, that merit re-consideration in light of the accumulated data. All of these reasons apply to a study of the Yagis as single units. 2-stack investigations--the original reason for going through the data compiling--will not be a part of these notes.

The raw data has resulted in the development of an extensive set of tables and graphs--so many that this document consists of 2 parts. This main document includes text, tables, and graphs belonging to the operating and physical characteristics of the two Yagi series. An appendix provides a collection of frequency-sweep graphs--2 per model--for the entire set of 72 models. Each document is too long for publication in any other venue than a web site. In addition, the number of individual graphics is so high that the PDF format is the only way to coalesce everything into a manageable number of site files. The collection of data is intended to serve as a reference for anyone who is seriously interested in long-boom Yagi design--whether or not the trimming Yagi is the type of array most desired. In fact, part of our commentary will include notes on some limitations of the trimming Yagi.

1. Background for the Yagi Series

The DL6WU Yagi series has evolved since the1980s. The current algorithms appear in a design program, dl6wu-gg.exe, which is available from the web site maintained by Ian White, G3SEK. See http://www.ifwtech.co.uk/g3sek. The program actually comes in two parts zipped together. Accompanying the DOS program is a text containing the original Basic code, as revised through 2003.

The design constraint for the series selected here is an element diameter of 4 mm (0.1575" or 0.00), a common European element size that is about midway between the commonly used U.S. rod sizes of 1/8" and 3/16". All dimensions used in the EZNEC models are in wavelengths. The series runs from 10 to 40 elements. The technique used in both the program and models is that all versions of the DL6WU Yagi shorter then 40 elements simply prune out the forward-most elements. **Table 1** shows the 432-MHz elements for the series.

DL6WU 432-MHz Yagi for 10-40 Elements									Table 1
Series WU10 to WU40			4 mm = 0.005764 wl						
Element	Boom Len	El. 1/2-L	El. Name	El. Len	Element	Boom Len	El. 1/2-L	El. Name	El. Len
1	0	0.243528	Reflector	0.487057	21	6.415029	0.193958	D19	0.387916
2	0.20001	0.239667	Driver	0.479333	22	6.81505	0.193396	D20	0.386792
3	0.274942	0.218066	D1	0.436132	23	7.215071	0.192863	D21	0.385726
4	0.455067	0.21553	D2	0.43106	24	7.614947	0.192359	D22	0.384717
5	0.670063	0.212951	D3	0.425901	25	8.014968	0.191883	D23	0.383766
6	0.919932	0.210501	D4	0.421002	26	8.414989	0.191408	D24	0.382815
7	1.200062	0.208325	D5	0.41665	27	8.815009	0.190975	D25	0.381951
8	1.499933	0.206437	D6	0.412874	28	9.21503	0.190543	D26	0.381086
9	1.814935	0.204809	D7	0.409618	29	9.61505	0.190125	D27	0.38025
10	2.145068	0.203368	D8	0.406736	30	10.01507	0.189736	D28	0.379472
11	2.490042	0.202085	D9	0.404171	31	10.41495	0.189347	D29	0.378694
12	2.850003	0.200947	D10	0.401894	32	10.81497	0.188987	D30	0.377973
13	3.224951	0.19991	D11	0.399819	33	11.21499	0.188627	D31	0.377253
14	3.615028	0.198958	D12	0.397917	34	11.61501	0.188281	D32	0.376561
15	4.015049	0.198094	D13	0.396188	35	12.01503	0.187949	D33	0.375898
16	4.41507	0.197287	D14	0.394574	36	12.41505	0.187618	D34	0.375236
17	4.814946	0.196523	D15	0.393046	37	12.81507	0.187301	D35	0.374602
18	5.214967	0.195831	D16	0.391663	38	13.21495	0.186998	D36	0.373996
19	5.614988	0.195169	D17	0.390337	39	13.61497	0.186696	D37	0.373391
20	6.015008	0.194535	D18	0.389069	40	14.01499	0.186407	D38	0.372815

To change element diameter, one needs to refigure the element lengths only. The element spacing remains constant for an element diameter between 0.001 and 0.02 λ. In fact, the program prescribes the element spacing in wavelengths in lines 2100 to 2130 of the program:

```
2100 ' Spacings for first 14 directors
2110 DATA 0.075, 0.180, 0.215, 0.250, 0.280, 0.300, 0.315
2120 DATA 0.330, 0.345, 0.360, 0.375, 0.390, 0.400, 0.400
2130 ' All spacings beyond D13 are equal to last entry ^
```

Elements 1-3, the reflector, driver, and first director, form the impedance-setting cell for the Yagis. The reflector-driver spacing is 0.2 λ, and the driver-director-1 spacing is 0.075 λ. The result is a wide-band Yagi capable of 2:1 50-Ω SWR coverage of the entire 70-cm band and beyond. Note that the director spacing from D13 (Element 15) onward is a constant 0.4 λ. In

ways that we shall address further on, the fact that the element spacing does not change with the element diameter--despite the 20:1 ratio between the fattest and thinnest elements--will make a difference to the data. Performance will remain acceptable across any chosen band, but there will be some shifting of peaks and nulls in the data sequence across the band with changes in element diameter.

There are at least two general methods of readjusting element lengths in response to a change in element diameter. One technique, explained in some detail in the RSGB volume *The VHF/UHF DX Book*, page 7-28, involves calculating a reactance for each element at its current diameter and length. Then one calculates a new length to yield the same reactance at the new diameter. The HAMCALC Basic suite of utilities has a program for this purpose. The program dl6wu-gg.exe uses a different technique of applying adjustment factors in steps of element diameter. Hence, it is less sensitive to small changes of diameter, but fully adequate to the design of DL6WU Yagis within the diameter limits.

```
2140 'First number in each data line is element diameter.
2150 'Next 4 numbers are K1-K4, used to determine element lengths.
2160 DATA .001,.4711,.018,.08398,.965
2170 DATA .003,.462,.01941,.08543,.9697
2180 DATA .005,.4538,.02117,.0951,1.007
2190 DATA .007,.4491,.02274,.08801,.9004
2200 DATA .01,.4421,.02396,.1027,1.038
2210 DATA .015,.4358,.02558,.1149,1.034
2220 DATA .02,.4268,.02614,.1112,1.036
```

The DL6WU Yagi series has rarely been matched for flexibility and for ease of home workshop replication. The design tolerates the normal home shop imprecision without giving up gain. In fact, the design criteria behind the Yagi series include good control of forward gain and of feedpoint impedance. Less controlled is the front-to-back ratio or the shape of the rearward lobes. These values fluctuate with the element diameter, the number of elements, and across the operating passband for any given version of the antenna. In a similar way, the feedpoint resistance and reactance also fluctuate, with resulting peaks and dips in the 50-Ω SWR across the passband.

The initial motivation for exploring the DL6WU Yagi series in detail arose in an exploration of the 2-stack behavior of these and other Yagis having long booms. Although the series allows exploration for boomlengths from 2 to 14 λ, the element spacing is too wide to detect certain properties at critical lengths. Therefore, I sought to develop a comparable Yagi series using closer element spacing. The design began with a 42-element 8-meter long design by David Tanner, VK3AUU. However, my modifications are too extensive to lay any responsibility on him for the final algorithms used to determine both element spacing and length. I first centered the impedance curve within the 70-cm band and increased the element diameter from the original 1/8" to 4 mm. I retained the general impedance-setting cell used in the original, with a reflector-driver spacing of 0.192 λ and a driver-director-1 spacing of 0.033 λ for a direct 50-Ω feed. In **Table 2**, you may note that the reflector is shorter than the driver, an ingredient in the impedance-setting function of the first 3 elements.

In the VK3AUU design, both the spacing of directors and their lengths are variable. Through a series of regression analyses, I gradually brought the frequency of maximum gain into closer alignment with the design frequency (432 MHz). The original design used a wider separation as one method of increasing the front-to-sidelobe ratio, that is, the ratio (in dB) between the main

forward lobe gain and the gain of the first and strongest forward sidelobe. The result of the modifications that I made included a higher and flatter gain curve within the 70-cm band and a weakening of forward sidelobe attenuation.

Series LB10 to LB50		El.Dia. 4mm = 0.005764 wl							Table 2
Element	Boom Len	El. 1/2-L	El. Name	El. Len	Element	Boom Len	El. 1/2-L	El. Name	El. Len
1	0	0.240724	Reflector	0.481448	26	6.214726	0.193614	D24	0.387228
2	0.191796	0.244811	Driver	0.489622	27	6.536565	0.193509	D25	0.387019
3	0.224914	0.221333	D1	0.442666	28	6.858905	0.193426	D26	0.386852
4	0.341075	0.218383	D2	0.436766	29	7.181598	0.193356	D27	0.386713
5	0.491915	0.215853	D3	0.431706	30	7.50457	0.193295	D28	0.38659
6	0.667335	0.213324	D4	0.426648	31	7.827819	0.193235	D29	0.38647
7	0.861946	0.210795	D5	0.42159	32	8.151421	0.193173	D30	0.386345
8	1.07171	0.208687	D6	0.417374	33	8.475526	0.193103	D31	0.386205
9	1.29494	0.20762	D7	0.41524	34	8.800355	0.193022	D32	0.386043
10	1.52962	0.206268	D8	0.412536	35	9.126208	0.192926	D33	0.385853
11	1.776853	0.204366	D9	0.408731	36	9.453458	0.192814	D34	0.385629
12	2.022582	0.202682	D10	0.405363	37	9.782551	0.192684	D35	0.385368
13	2.279996	0.201199	D11	0.402397	38	10.11401	0.192533	D36	0.385067
14	2.547825	0.199901	D12	0.399801	39	10.44843	0.192362	D37	0.384725
15	2.824879	0.198772	D13	0.397543	40	10.78649	0.192171	D38	0.384342
16	3.110038	0.197796	D14	0.395592	41	11.12892	0.19196	D39	0.38392
17	3.402258	0.19696	D15	0.39392	42	11.47655	0.191731	D40	0.383461
18	3.700572	0.196249	D16	0.392499	43	11.83027	0.191485	D41	0.382969
19	4.004083	0.195651	D17	0.391301	44	12.19106	0.191225	D42	0.382449
20	4.311973	0.195151	D18	0.390303	45	12.55995	0.190954	D43	0.381908
21	4.623496	0.194739	D19	0.389479	46	12.93806	0.190677	D44	0.381353
22	4.93798	0.194403	D20	0.388807	47	13.3266	0.190397	D45	0.380793
23	5.25483	0.194133	D21	0.388265	48	13.72681	0.19012	D46	0.380239
24	5.573523	0.193917	D22	0.387834	49	14.14005	0.189851	D47	0.379702
25	5.893613	0.193747	D23	0.387494	50	14.56774	0.189597	D48	0.379194

The table shows a continuous decrease in the director lengths. However, the original design used some matched pairs of directors. The smoothed curves for both element spacing and element length are a function of the regression analyses.

The overall boomlength for 50 elements is just above 14.5 λ, comparable to the 40-element DL6WU series. For purposes of data gathering convenience, the DL6WU series will use Yagis from 10 to 40 elements, while the test series (labeled LB for "long-boom") will use 10 through 50 elements. However, note that 10 elements in the test series require only a 1.5 λ boom, whereas the same number of elements in the DL6WU series needs a 2.15 λ boom. **Fig. 1** compares the boomlength vs. the number of elements for the two test series.

The differences in the design algorithms between the DL6WU and test series become evident in **Fig. 2**. The curvature of element lengths closely reflects the shape of normalized curves when each series is subjected to regression analysis. The DL6WU curve shows a single curvature characteristic. In contrast, the test series shows multiple steps. Had I carried out the process further to bring the peak gain and design frequencies into exact alignment, the right end of the curve would be shallower than it is on the graph. However, the characteristics of the two series are sufficiently similar so that additional curve adjustment seemed superfluous. The graph includes only directors. Beyond the 20th element, the test-series elements are universally longer than the corresponding elements in the DL6WU series, even when adjusted for their position in wavelengths.

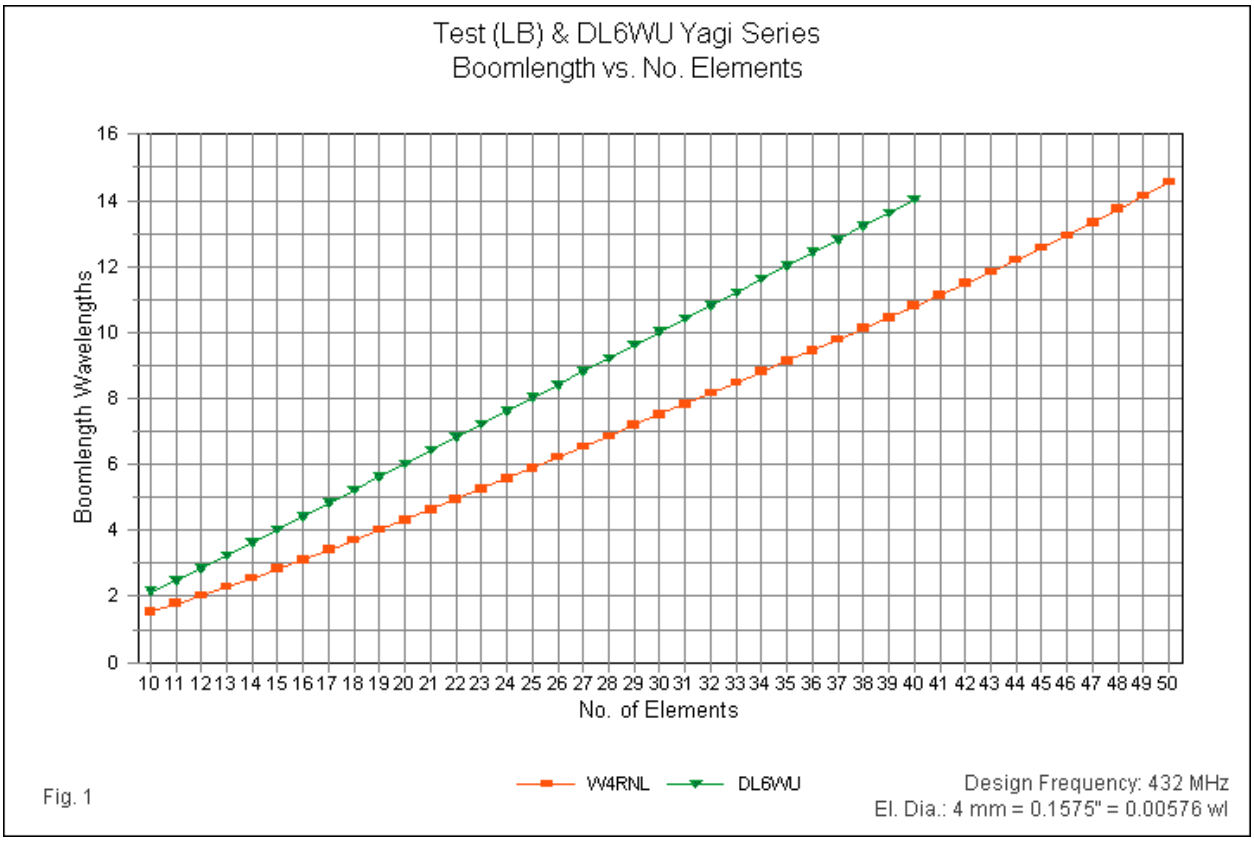
Test (LB) & DL6WU Yagi Series
Boomlength vs. No. Elements
Boomlength Wavelengths
No. of Elements
W4RNL
DL6WU
Design Frequency: 432 MHz
El. Dia.: 4 mm = 0.1575" = 0.00576 wl

Fig. 1

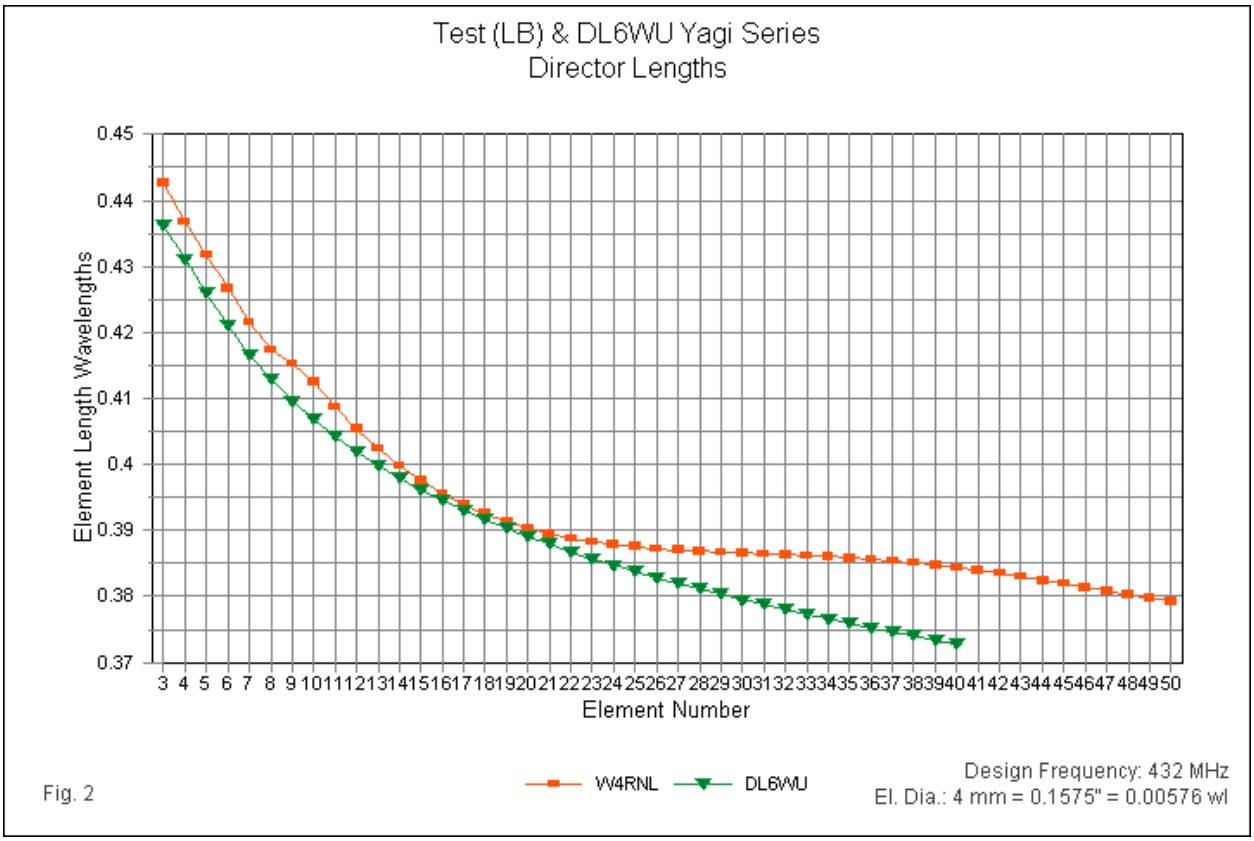
Test (LB) & DL6WU Yagi Series
Director Lengths
Element Length Wavelengths
Element Number
W4RNL
DL6WU
Design Frequency: 432 MHz
El. Dia.: 4 mm = 0.1575" = 0.00576 wl

Fig. 2

Fig. 3

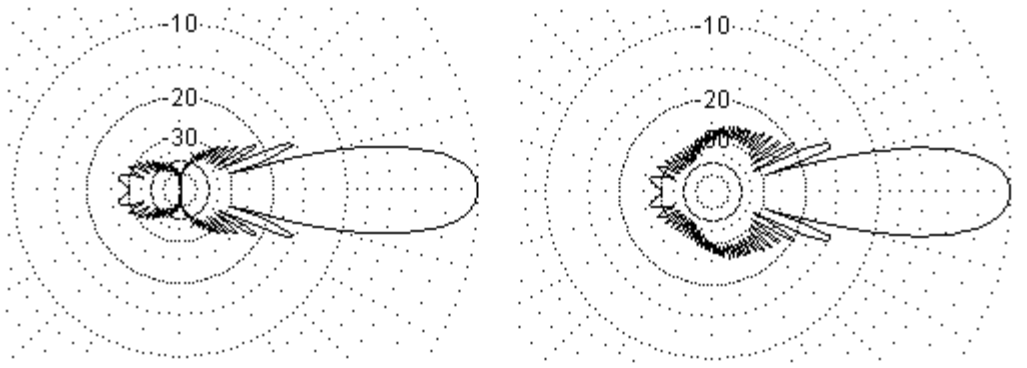

DL6WU-40 Elements: Free-Space Patterns

Fig. 3 shows both the E-plane (azimuth) and H-plane (elevation) patterns in free space of the longest DL6WU Yagi in the series. If the scale were larger, one could count the number of forward and rearward sidelobes on each side of the pattern centerline. The number would approximately equal the number of wavelengths occupied by the boom. The design criteria used in the development of the series do not include sidelobe suppression. (Sidelobe attenuation involves the simple reduction in sidelobe strength. Sidelobe suppression involves not only reductions in sidelobe strength, but as well, a reduction in the number of sidelobes on each side of the pattern centerline. Sidelobe suppression is a characteristic of the OWA series of Yagis, which has not been developed to the boomlength required for the extended 2-stack studies. The technique involves careful adjustment to the length of the second and third directors, in relationship to the elements in the impedance-setting cell.)

Sidelobes and Beamwidth				Maximum-Length Yagis			
Yagi	Gain 432	Pk Gn Fq	Pk Gain	H BW	H F/SL	V BW	V F/SL
WU-40	20.4	441	21	18.4	15.43	18.8	14.6
Trial-1-50	20.53	445.5	20.77	19.4	17.71	19.8	16.84
Trial-2-50	20.67	441	21	18.4	16.47	18.8	15.66
Final-50	21.1	436	21.2	16.8	14.37	17	13.62
Notes:							
Gain 432 = Free-Space Gain at 432 MHz in dBi							
Pk Gn Fq = Peak gain frequency in MHz							
Pk Gain = Gain at Pk Gn Fq							
H BW = Horizontal beamwidth in degrees							
H F/SL = Horizontal front-to-sidelobe ratio in dB							
V BW = Vertical beamwidth in degrees							
V F/SL = Vertical front-to-sidelobe ratio in dB							Table 3

Table 3 shows a sample of the relationship among 3 factors, a relationship that first appeared in the development of the final test series of 50-element Yagis. All 4 listed Yagis use boomlengths above 14 λ. The trial and final 50-element Yagis are slightly longer than the DL6WU 40-element version. The test series brought the frequency of maximum gain into closer alignment with the design frequency, with resulting increases in both design-frequency and peak gain. Trial 2 has the same maximum gain and the same horizontal and vertical beamwidth values as the DL6WU

representative. However, the front-to-sidelobe ratios are slightly better. The final version brings the peak and design frequencies closest together, with a small gain increase and a significant weakening of the front-to-sidelobe ratio. **Fig. 4** shows the azimuth and elevation patterns for the 3 test-series trials at the 50-element, 14.5-λ boom size.

Fig. 4

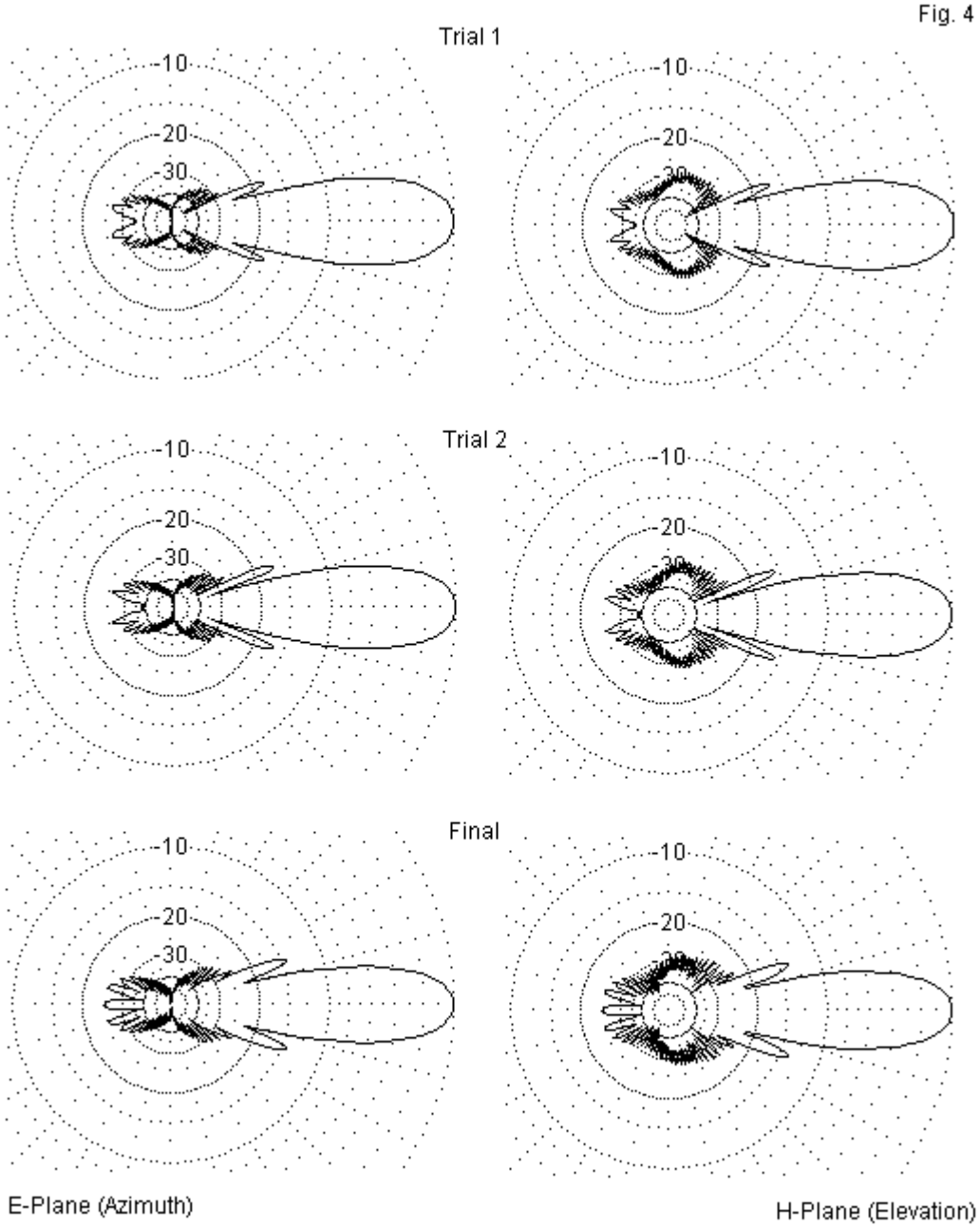

Long-Boom Test (LB) Series Patterns: 50 Elements

There are a number of beamwidth estimation equations floating around, all of which are based on the gain of the subject antenna. None of these equations takes into account the relationship of the beamwidth to the front-to-sidelobe ratio. However, the sample in **Table 3** shows a factor that we shall have occasion to examine in more detail. The beamwidth and the forward

sidelobe strength are inversely related. Otherwise expressed, the wider the beamwidth, the higher the front-to-sidelobe ratio. Since there are other design factors built into the final value for each of these figures, we do not find a direct numerical relationship between the beamwidth and the sidelobe strength, but only a general trend. Compare the DL6WU example with Trial 2, where both of the beamwidth values are the same, but the front-to-sidelobe values differ by about 1 dB in each case--more than the difference in gain at 432 MHz. As well, vertical front-to-sidelobe values are lower in the less controlled H-plane of the array.

The data here--and data yet to emerge--strongly suggest that some traditional methods of estimating beamwidth for long-boom Yagis need revision. OWA Yagis that both suppress and attenuate sidelobes typically show wider beamwidths than trimming Yagis. As well, there tends to be a greater difference in the horizontal and vertical beamwidths. As modern design techniques uncover additional Yagi sequences, we shall likely also uncover further deviations from the traditional equations.

Single-Unit Performance at the Design Frequency

As a prelude to 2-stack studies, I had to check the performance of each possible Yagi length in both series at the design frequency. In both tabular and graphical form, the exercise shows some interesting patterns. **Table 4** shows the DL6WU data in raw form.

DL6WU 40-Element Series for Detailed Study of Stack Behavior										Table 4
Single-Unit Free-Space Performance at 432 MHz										
Elements	Bm-Ln	Gain	180 F-B	H BW	H F/SL	V BW	V F/SL	FP Resis	FP React	SWR-50
10	2.145068	13.88	31.92	37.6	19.08	41.6	13.4	49.65	13.75	1.317
11	2.490042	14.26	16.96	35.8	18.19	39	13.32	46.34	-2.133	1.092
12	2.850003	14.76	15.49	34	17.81	36.6	13.63	60.77	-7.831	1.273
13	3.224951	15.28	19.31	32.4	17.82	34.8	14.14	67.77	7.426	1.39
14	3.615028	15.69	28.63	31.2	17.78	33.2	14.5	55.32	14.59	1.342
15	4.015049	15.99	21.14	30	17.58	31.8	14.62	46.94	8.065	1.195
16	4.41507	16.27	17.54	29	17.4	30.6	14.69	47.93	-0.747	1.046
17	4.814946	16.59	17.68	28	17.32	29.5	14.88	56.06	-4.267	1.15
18	5.214967	16.92	21.43	27.2	17.37	28.6	15.08	62.63	2.498	1.258
19	5.614988	17.21	33.2	26.6	17.33	27.6	15.19	57.93	10.14	1.269
20	6.015008	17.43	24.37	25.8	17.16	26.8	15.17	50.63	8.346	1.181
21	6.415029	17.61	19.8	25.2	16.96	26.2	15.11	49.36	2.042	1.044
22	6.81505	17.82	19.51	24.6	16.85	25.6	15.11	54.25	-1.789	1.093
23	7.215071	18.06	22.92	24	16.77	24.8	15.15	59.8	1.5	1.198
24	7.614947	18.28	35.99	23.6	16.68	24.4	15.17	58.13	7.621	1.229
25	8.014968	18.45	26.69	23	16.57	23.8	15.08	52.51	7.764	1.172
26	8.414989	18.59	21.48	22.6	16.38	23.4	14.99	50.53	3.24	1.067
27	8.815009	18.74	20.94	22.2	16.32	22.8	15.02	53.68	-0.269	1.074
28	9.21503	18.92	24.14	21.8	16.24	22.4	14.96	58.18	1.445	1.166
29	9.61505	19.09	37.43	21.4	16.16	22	14.96	57.81	6.209	1.204
30	10.01507	19.23	28.42	21.2	16.04	21.6	14.86	53.52	7.112	1.166
31	10.41495	19.35	22.83	20.8	15.98	21.2	14.88	51.42	3.796	1.083
32	10.81497	19.47	22.14	20.4	15.88	21	14.79	53.55	0.724	1.073
33	11.21499	19.61	25.2	20.2	15.91	20.6	14.84	57.21	1.637	1.148
34	11.61501	19.75	38.02	20	15.76	20.4	14.75	57.4	5.389	1.186
35	12.01503	19.87	29.7	19.6	15.72	20	14.72	54.09	6.55	1.16
36	12.41505	19.97	23.93	19.4	15.67	19.8	14.75	52.08	4.062	1.093
37	12.81507	20.07	23.15	19	15.58	19.6	14.66	53.56	1.402	1.077
38	13.21495	20.18	26.12	18.8	15.57	19.2	14.66	56.58	1.876	1.137
39	13.61497	20.3	38.19	18.6	15.55	19	14.71	57.02	4.887	1.173
40	14.01499	20.4	30.61	18.4	15.43	18.8	14.6	54.4	6.095	1.155

The comparable data for the test series appears in **Table 5**.

LB10-LB50 Yagi Series										Table 5
Single-Unit Free-Space Performance at 432 MHz										
Elements	Bm-Ln	Gain	180 F-B	H BW	H F/SL	V BW	V F/SL	FP Resis	FP React	SWR-50
10	1.52962	12.7	17.6	41	19.65	46.4	12.41	40.92	4.399	1.249
11	1.77685	13.28	16.96	38.6	18.23	43	12.43	61.46	-15.72	1.418
12	2.02258	13.64	19.6	37.6	18	41	12.73	45.55	6.406	1.177
13	2.28	14.08	17.04	35.4	17.21	38.8	12.71	53.05	-14.81	1.34
14	2.54783	14.46	25.31	34.4	17.31	37.2	13.22	54.06	7.202	1.172
15	2.82488	14.79	16.19	33	16.9	35.6	13.27	45.77	-9.12	1.233
16	3.11004	15.18	34.39	32	17.15	34.4	13.84	61.69	-1.357	1.236
17	3.40226	15.45	18.46	31	17.17	33.2	14.12	45.65	0.014	1.095
18	3.70057	15.78	21.34	30.2	17.3	32	14.53	54.47	-10.62	1.246
19	4.00408	16.08	25.33	29.4	17.66	31.2	15.06	55.04	3.434	1.123
20	4.31197	16.32	18.76	28.6	17.73	30.2	15.31	46.42	-4.955	1.135
21	4.6235	16.61	28.14	28	18.07	29.4	15.8	57.77	-7.062	1.215
22	4.93798	16.85	22.1	27.2	18.29	28.6	16.16	51.52	2.586	1.061
23	5.25483	17.07	20.12	26.6	18.37	27.8	16.39	48.2	-6.76	1.153
24	5.57352	17.32	36.5	26	18.64	27.2	16.78	58.02	-4.575	1.187
25	5.89361	17.52	21.34	25.4	18.68	26.6	16.88	50.18	1.421	1.029
26	6.21472	17.72	21.56	24.8	18.67	25.8	16.98	49.5	-7.136	1.159
27	6.53657	17.94	37.54	24.4	18.73	25.2	17.15	57.63	-3.193	1.166
28	6.85891	18.11	21.18	23.8	18.54	24.8	17.01	49.57	0.533	1.014
29	7.1816	18.29	22.97	23.4	18.42	24.2	16.98	50.45	-7.504	1.161
30	7.50457	18.49	33.15	23	18.3	23.6	16.88	57.17	2.278	1.151
31	7.82782	18.64	21.23	22.4	17.98	23.2	16.65	49.2	-0.183	1.017
32	8.15142	18.81	24.43	22	17.83	22.6	16.51	51.21	-7.562	1.163
33	8.47553	18.98	30.48	21.6	17.53	22.2	16.29	56.73	-1.638	1.139
34	8.80036	19.11	21.4	21.2	17.22	21.8	16	49	-0.722	1.025
35	9.12621	19.26	25.69	20.8	16.98	21.4	15.84	51.68	-7.507	1.163
36	9.45346	19.42	29.4	20.5	16.7	21	15.56	56.46	-1.438	1.132
37	9.78155	19.54	21.68	20.2	16.43	20.6	15.37	49.09	-0.867	1.026
38	10.114	19.68	26.02	19.8	16.17	20.2	15.12	51.44	-7.351	1.159
39	10.4484	19.83	30.71	19.4	15.97	20	14.92	56.57	-2.19	1.139
40	10.7865	19.94	22.09	19.2	15.67	19.6	14.7	49.88	-0.156	1.004
41	11.1289	20.06	24.66	18.8	15.48	19.2	14.51	50.03	-6.542	1.14
42	11.4766	20.2	40.83	18.6	15.35	19	14.39	56.38	-4.713	1.161
43	11.8303	20.32	23.57	18.4	15.08	18.6	14.16	52.76	0.781	1.057
44	12.1911	20.42	22.45	18	14.92	18.4	14.03	48.44	-3.188	1.075
45	12.56	20.54	28.54	17.8	14.86	18.2	13.97	52.09	-7.434	1.163
46	12.9381	20.67	34.4	17.6	14.66	18	13.84	56.76	-3.973	1.158
47	13.3266	20.78	23.92	17.4	14.53	17.6	13.71	53.92	0.908	1.08
48	13.7268	20.88	21.71	17.2	14.5	17.4	13.68	49.07	-0.235	1.02
49	14.1401	20.99	22.34	17	14.43	17.2	13.68	47.69	-4.435	1.108
50	14.5677	21.1	24.84	16.8	14.37	17	13.62	49.69	-8.118	1.177

Perhaps the first question to be answered is whether--given design differences already outlined--the two series of Yagis have truly comparable performance for any given boomlength. Since gain is one of the two main controlled design elements (the other being the feedpoint impedance), we may compare gain vs. boomlength. However, only at certain boomlengths do the two series of Yagis have elements that may serve as the final forward director. **Table 6** summarizes the data for these selected boomlengths--which are close but not exact. Nevertheless, the gain values at the design frequency are sufficiently close to declare the 2 series to be comparable. The wider difference between the design and peak gain frequencies for the DL6WU series may require you to use a simple averaging of the 2 gain values to clearly see a correlation with the test-series data. Differences remain, and these shall appear as we explore the patterns of data in greater detail.

Comparison of BoomLength and Gain for DL6WU and Test Series Yagis									Table 6
Test Series					DL6WU Series				
No. of El.	Bm Ln	Gain	Pk Gain	Pk Gn Fq	No. of El.	Bm Ln	Gain	Pk Gain	Pk Gn Fq
15	2.824879	14.79	14.81	430	12	2.850003	14.76	14.95	441
19	4.004083	16.08	16.08	432	15	4.015049	15.99	16.25	437
23	5.25483	17.07	17.07	432	18	5.214967	16.92	17.19	441
29	7.181598	18.29	18.31	433	23	7.215071	18.06	18.44	440
34	8.800355	19.11	19.17	435	27	8.815009	18.74	19.19	439
39	10.44843	19.83	19.86	434	31	10.41495	19.35	19.8	442
47	13.3266	20.78	20.83	434	38	13.21495	20.18	20.74	440
Notes:				Gain = Gain at 432 MHz					
No. of El. = Number of Elements				Pk Gain = Peak Gain					
Bm Ln = Boomlength in wavelengths				Pk Gn Fq = Peak Gain Grequency in MHz					

As we add elements to the DL6WU series of Yagis, the gain increases in predictable ways. **Fig. 5** shows the gain curve as a function of the number of elements, since plotting it as a function of boomlength is not feasible in any ready way. However, the tabular data allows correlation of each element number and its corresponding boomlength. The correlative gain curve for the test series appears in **Fig. 6**. The curve is equally smooth. Its range is slightly greater, since a 10-element array represents a shorter boomlength on the test series than for the DL6WU series. The smoothness of both curves tends to confirm that each series is an adequate trimming Yagi design.

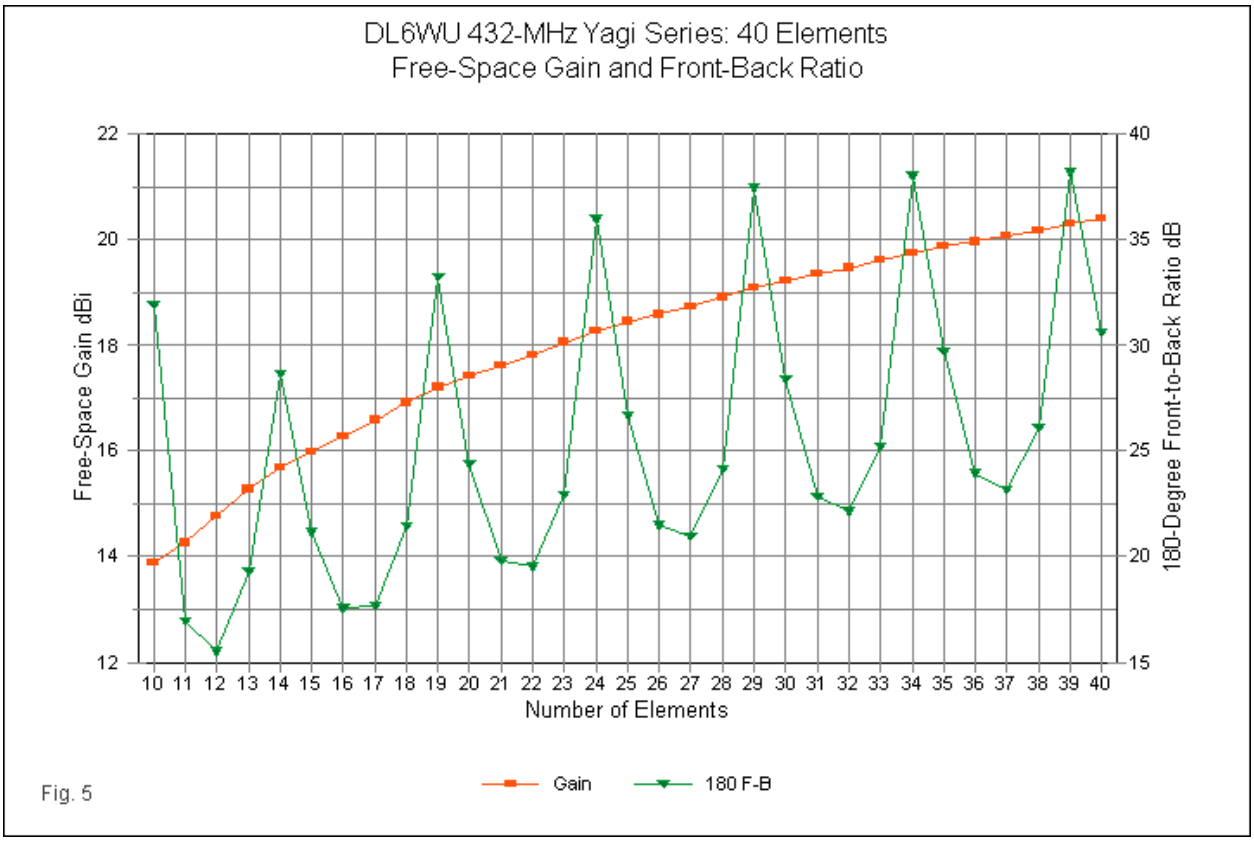

Fig. 5

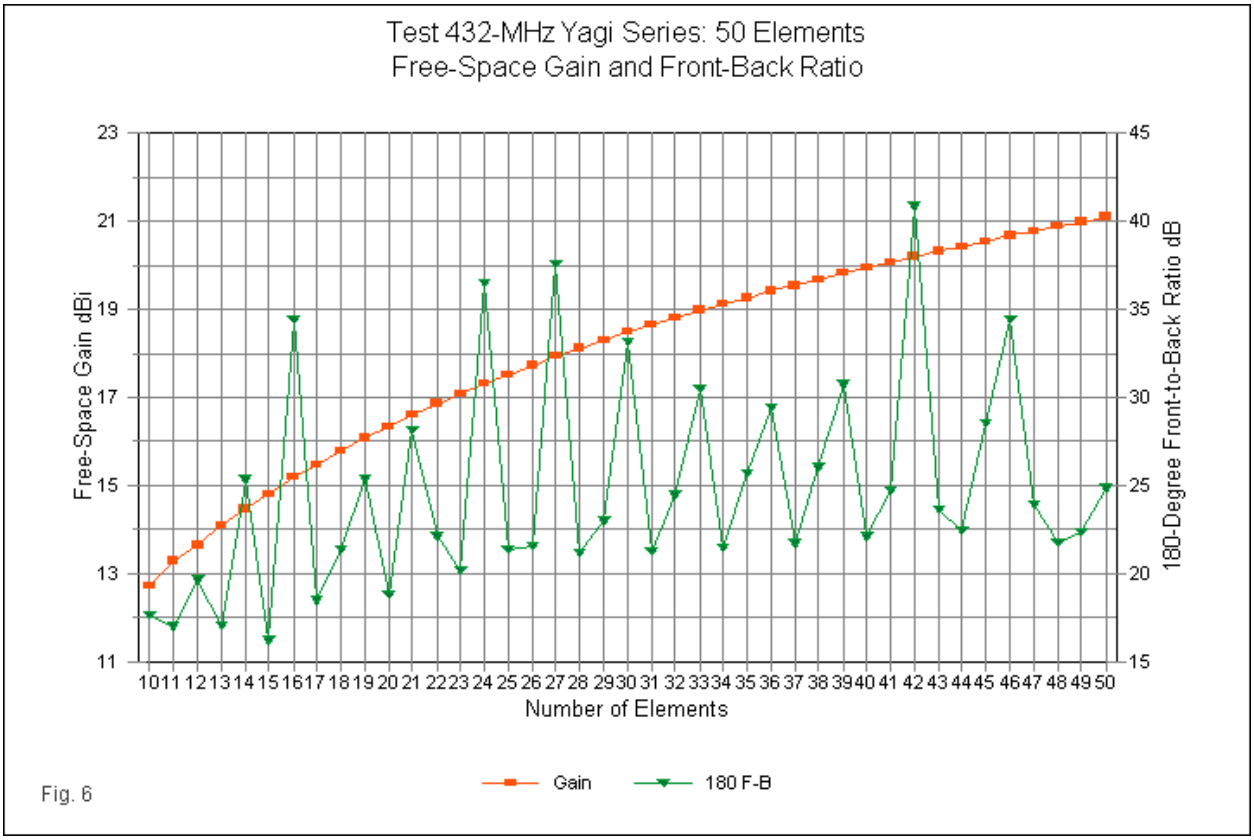

Fig. 6

More interesting are the respective 180° front-to-back curves. The DL6WU shows an average spacing of about 5 elements between front-to-back peak values occurring at the design frequency. If the undulations in the appearance of a front-to-back peak were a function of boomlength alone, we would expect to see a greater number of elements between peaks in the test series. However, precisely the opposite is true. The average spacing between front-to-back peaks is about 3 new elements. The actual figure grows from about 2 new elements at the short end of the boomlength range to 4 new elements at the high end. However, the test series does not use a constant spacing between elements. Instead, the element spacing nearly doubles across the range of elements in the graph. The spacing between elements 10 and 11 is about 0.247 λ, while the spacing between elements 49 and 50 is 0.428 λ. In the DL6WU design, the spacing past element 12 is a constant 0.4 λ. (One consequence of this difference is that past the 47th element, the test series Yagis grow in boomlength faster than the DL6WU series. This fact limits the utility of the test series past 50 elements for 2-stack testing, since the boomlength increment no longer permits finer gradations of array length vs. the required stacking space for maximum stack gain.)

Each Yagi series presents an interesting pattern of both horizontal (E-plane) and vertical (H-plane) beamwidth values, where beamwidth is the angular distance between half-power points in degrees. We may contrast the horizontal and vertical beamwidth curves within each series, as done in **Fig. 7** for the DL6WU series and in **Fig. 8** for the test series. As well, we may compare the patterns between the two series both as a whole and individually for the horizontal and the vertical curves. Since beamwidth values appear in EZNEC only to 1 decimal place and often in increments of 0.2° minimum, the curves will not be perfectly smooth. However, as the figures show, the departures from truly smooth curves are very small.

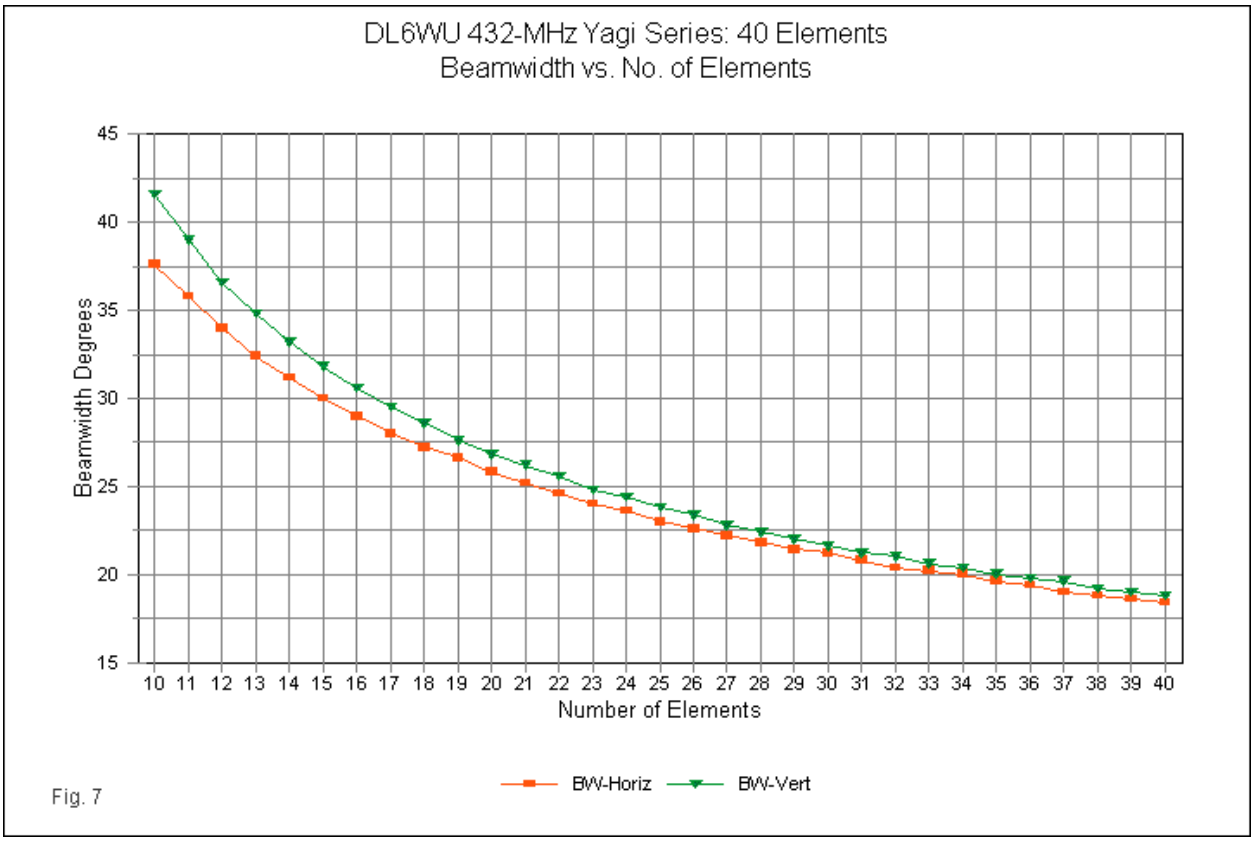
DL6WU 432-MHz Yagi Series: 40 Elements
Beamwidth vs. No. of Elements
Beamwidth Degrees
45
40
35
30
25
20
15
10 11 12 13 14 15 16 17 18 19 20 21 22 23 24 25 26 27 28 29 30 31 32 33 34 35 36 37 38 39 40
Number of Elements
BW-Horiz
BW-Vert

Fig. 7

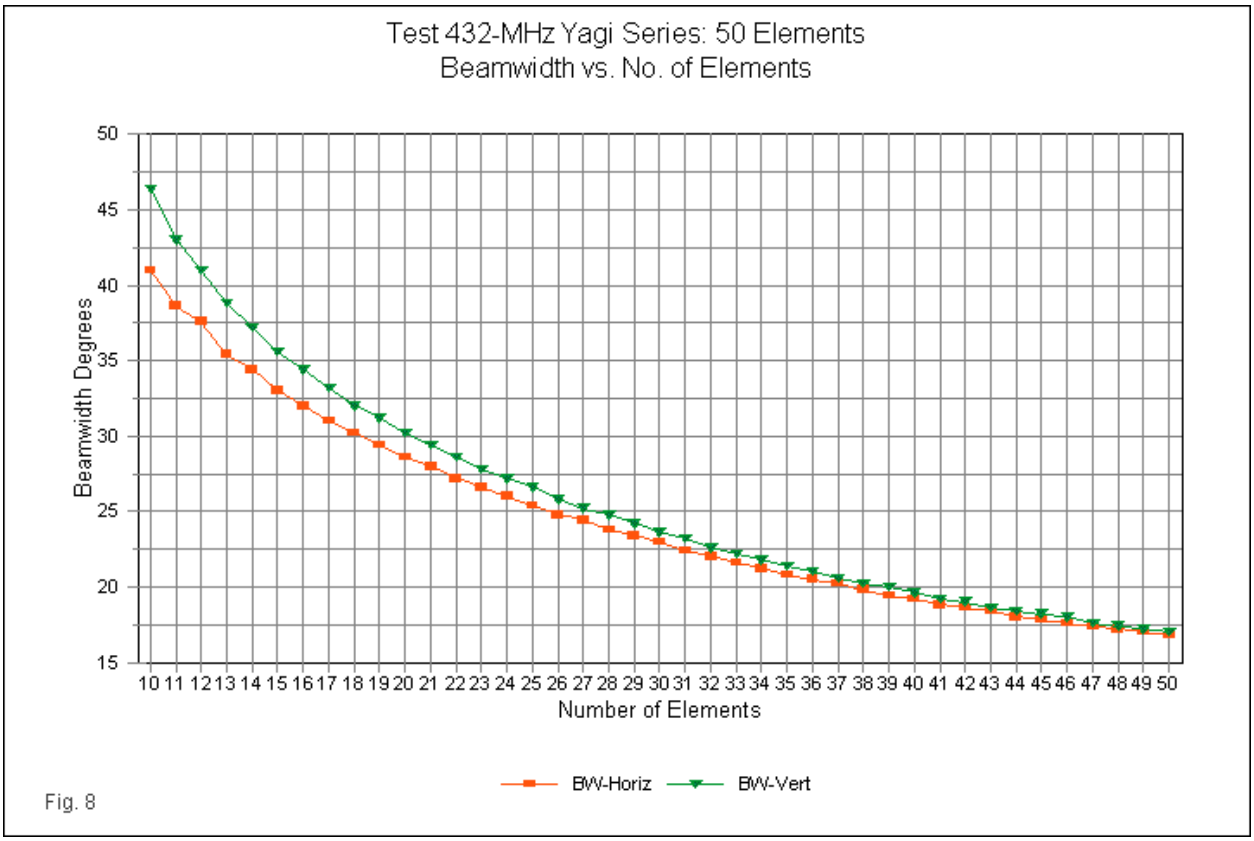
Test 432-MHz Yagi Series: 50 Elements
Beamwidth vs. No. of Elements
Beamwidth Degrees
50
45
40
35
30
25
20
15
10 11 12 13 14 15 16 17 18 19 20 21 22 23 24 25 26 27 28 29 30 31 32 33 34 35 36 37 38 39 40 41 42 43 44 45 46 47 48 49 50
Number of Elements
BW-Horiz
BW-Vert

Fig. 8

The two sets of curves show a relatively constant proportion between the narrower horizontal value and the wider vertical value. The data suggest that beamwidth is less a function of boomlength than of gain at the frequency of interest--in this case, 432 MHz. The DL6WU array at the 40th element shows a free-space gain of 20.4 dBi and a boom length just over 14 λ. For the same 18.4° horizontal beamwidth in the test series, we must look at the data for 43 elements, where the boomlength is only 11.8 λ, but the gain is 20.32 dBi.

As suggested earlier, the beamwidth and the front-to-sidelobe ratio are strongly connected, but not as a set of variables that are independent of others. The 43-element test-series Yagi has a horizontal front-to-sidelobe ratio of 15.08 dB. The 40-element DL6WU array has a horizontal front-to-sidelobe ratio of 15.43 dB, a value that is about half way between the values for the 41- and 42-element test series Yagis.

Unlike the relatively smooth beamwidth curves for both series, the front-to-sidelobe curves--when recorded vs. the number of elements--are far less smooth. **Fig. 9** shows the curves for the DL6WU series of Yagis. Ignoring the minor undulations for the moment, the DL6WU curve for the H-plane shows a peak at 19 elements, where the boomlength is 4.42 λ and the gain is 16.08 dBi. The vertical plane curve is relatively flat until about 24 elements (gain 18.28 dBi, boomlength 7.61 λ). For further increases in the boomlength and the number of elements, the horizontal and vertical front-to-sidelobe ratio curves track reasonably well. Below 18 elements, the two curves are almost complements to each other in their divergence, with similar rates of change although in opposite directions. The minor undulations in value in each curve show a correspondence to each other as well as to the number of elements in the array. They are wider for shorter boomlengths and numbers of elements and more closely spaced at the long end of the length scale.

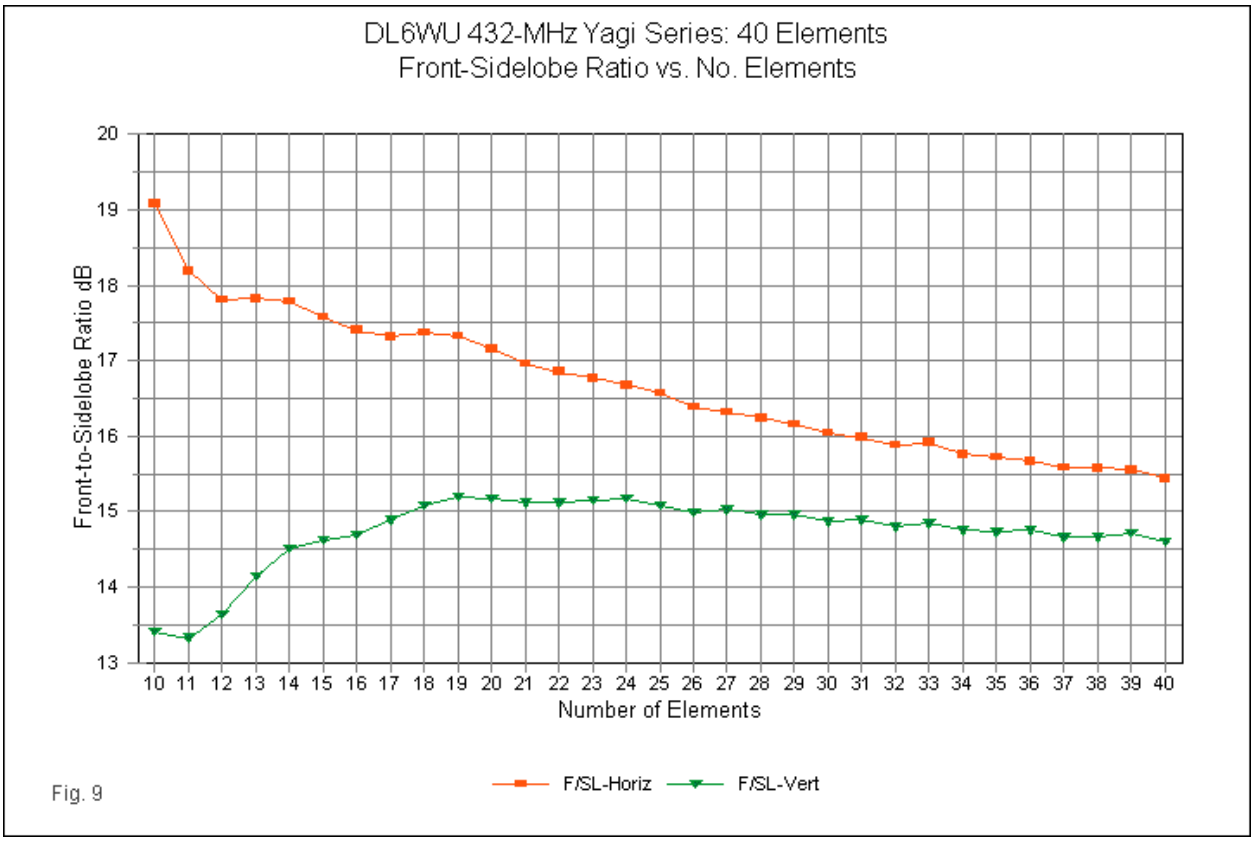

Fig. 9

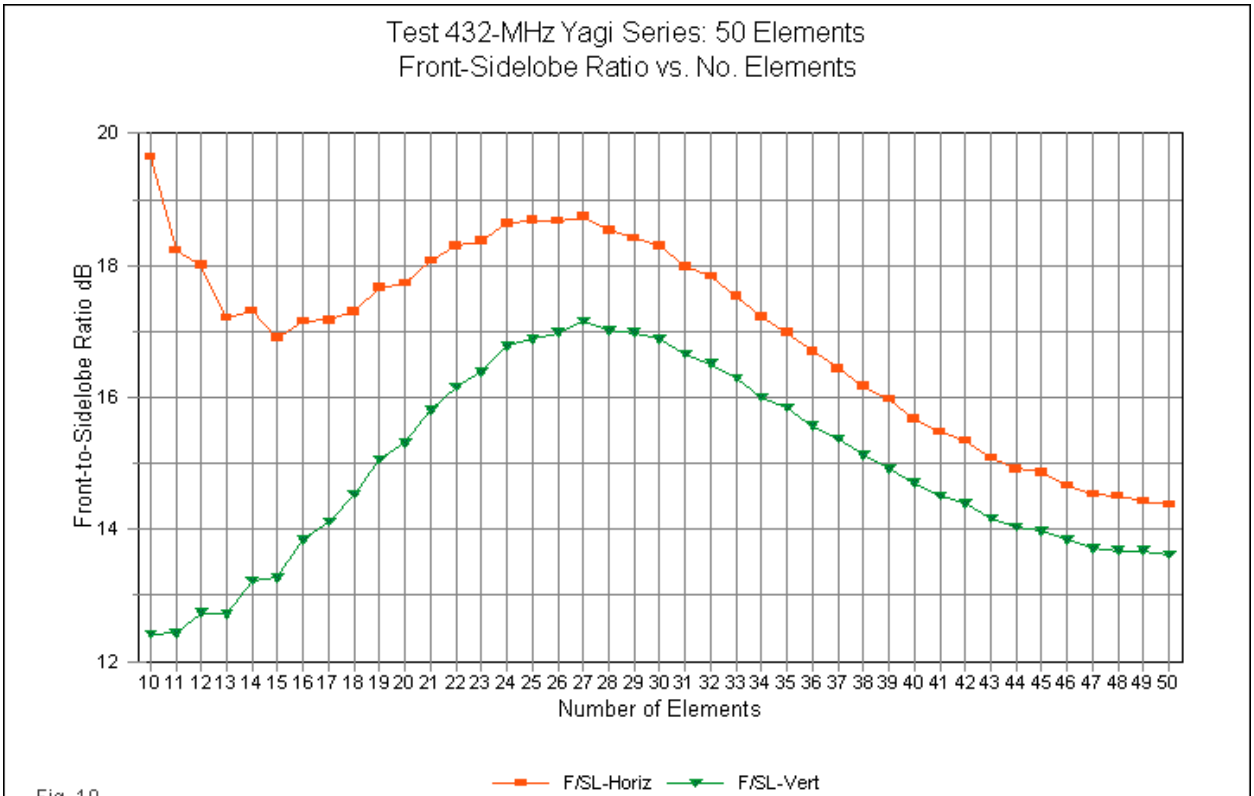

Fig. 10

The behavior of the front-to-sidelobe ratios for the test series shows both similarities and departures from the DL6WU patterns. **Fig. 10** plots the relevant data. The divergence of horizontal and vertical ratios appears at the short end of the boomlength range. However, by the 15th element (gain 14.79 dBi, boomlength 2.82 λ), the two curves begin to track each other. Unlike the DL6WU curve, the initial tracking is upward in value until both curves reach a peak at a length of 27 elements (gain 17.94 dBi, boomlength 6.54 λ). The peak values of front-to-sidelobe ratio for the test series exceed the corresponding peaks in the DL6WU series by about 1.5 dB in the horizontal plane and nearly 2 dB in the vertical plane. The test series curves past the peak value track each other well, with a gradual flattening of the curve at the longest boomlengths. However, at a boomlength of 14 λ or more, the DL6WU values exceed those of the test series by about 1 dB. It is likely that the contrast in element spacing algorithms has something to do with the differences between the curves in the upper half of the total range of elements. The constant DL6WU increment between new directors yields a shallower curve downward in both planes. The variable test series element spacing produces a higher peak with more closely spaced elements, but ends up with lower front-to-sidelobe ratio values as the element spacing reaches and exceeds the DL6WU value. However, it is unlikely that the relationships are exclusive. Like the DL6WU series, the test series of Yagis shows minor tracking undulations in the curves, although the peak-to-null ranges and the element spans of the undulations are both smaller.

Plots of the feedpoint resistance and reactance for each series are especially interesting. **Fig. 11** tracks the resistance and reactance values for each size of DL6WU array. **Fig. 12** performs the same function for the test series of Yagis. Once more, we shall look at each graph internally and also compare the characteristics of the two series.

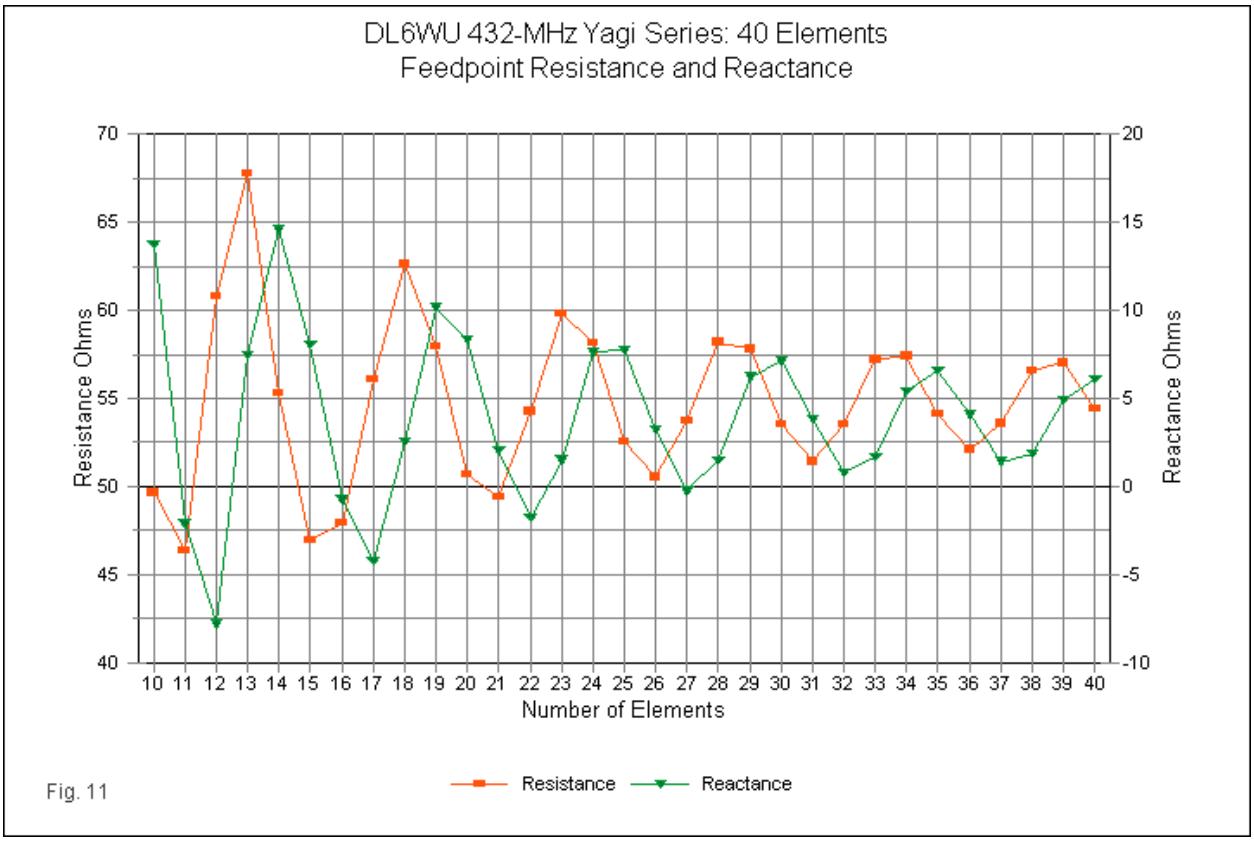
DL6WU 432-MHz Yagi Series: 40 Elements
Feedpoint Resistance and Reactance
Resistance Ohms
Reactance Ohms
Number of Elements
Resistance
Reactance

Fig. 11

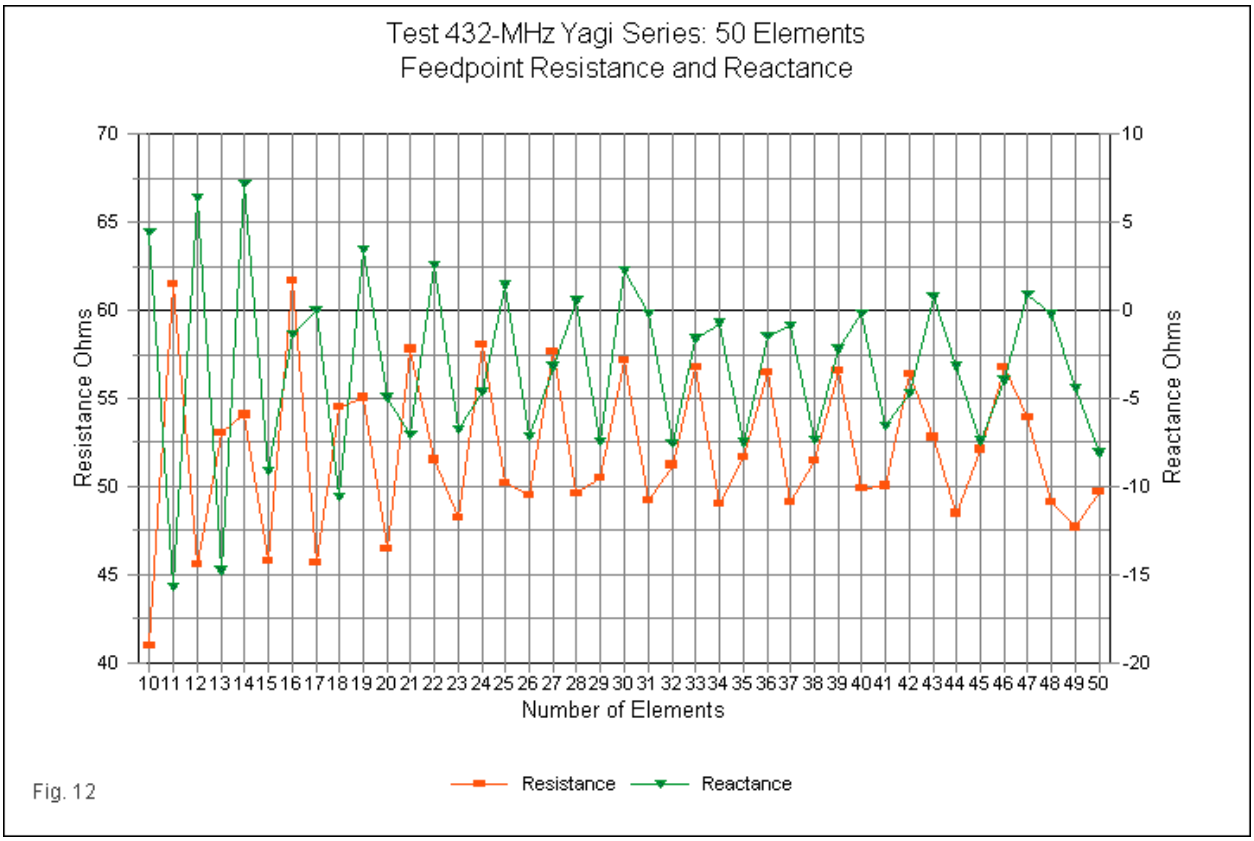
Test 432-MHz Yagi Series: 50 Elements
Feedpoint Resistance and Reactance
Resistance Ohms
Reactance Ohms
Number of Elements
Resistance
Reactance

Fig. 12

The DL6WU chart shows clearly that peak values of resistance and peak values of inductive reactance do not occur together. Likewise, minimum resistance values and peak values of capacitive reactance do not occur together. The reactance values peak at an array length just over 1 element (about 0.4 λ) larger than the resistance maximums and minimums. As we shall see, this offset has beneficial effects for the SWR curve, generally freeing it from major spikes. The relatively constant spacing of each new element as the Yagi series grows results in a nearly constant spacing between all maximums and minimums of just over 5 elements per cycle.

We noted in connection with the front-to-back ratio graphs that there was no correspondence between boomlength and the spacing between peaks in that value as we change from one set of Yagis to the other. If anything, the reverse occurs: the closer the elements to each other, the fewer new elements between peaks in front-to-back ratio value. A similar phenomenon applies to the resistance and reactance curves across the range of the test series Yagis in comparison to the DL6WU series. Like the DL6WU series, the reactance shows its peaks about 1 element longer than it shows its resistance maximum and minimum values. However, the maximum and minimum positions are only an average of 3 new elements apart. Since the element spacing is variable, the test series shows a range of distances between peaks that varies from 2 new elements on short-boom versions to 4 new elements for the longest booms. The parallel between front-to-back values and resistance and reactance maximums and minimums suggests that there is a relationship among these characteristics of long-boom Yagis. However, we cannot directly derive even tentative formulations of that relationship, since the integer requirement for new element addition prevents us from seeing the precise position of the maximum and minimum values that any of these parameters might reach. Many of the maximums and minimums show nearly flat curves to adjacent values, suggesting that the true maximum or minimum is somewhere between. However, for models of either Yagi series, it is not possible to add fractional elements.

To what--if any--degree the impedance-setting cell differences play a role in the behavior of the front-to-back and the resistance-reactance curves is an interesting question beyond the scope of this accumulation of data. It may be possible to graft the director set from each series onto the first 6 to 8 elements of the other series and check the behavior in the relevant categories. We would then have 2 new hybrid series of Yagis for analysis. The reliability of the hybrids would depend in part on the ability of each to replicate key elements in the trimming Yagi design criteria. As noted in the commentary on the physical properties of the 2 series, the DL6WU Yagis use a 0.2-λ reflector-driver spacing with a 0.075-λ driver-director-1 spacing. The DL6WU reflector is "standard," that is, longer than the driver and electrically close to ½ λ. The test series uses the VK3AUU cell in which the reflector-driver spacing is about 0.192 λ, but the driver-director-1 spacing is much closer at 0.033 λ. The reflector is shorter than the driver. One would need to analyze the progression of directors in order to assure that the core cell onto which one grafts the remaining directors is sufficient to retain the impedance-setting characteristics of the original series.

The resistance and reactance behavior has consequences for the 50-Ω SWR values exhibited by the two series of Yagis at the design frequency. In general, the offset between peak reactance values and maximum and minimum resistance values yields a smoother SWR curve than might otherwise occur. **Fig. 13** tracks the SWR values for the DL6WU series. The test-series SWR values appear in **Fig. 14**. Separate graphs are required for each series so that the range of boomlengths may correspond, at least roughly. The shortest test-series boomlength is shorter than the DL6WU 10-element counterpart, and the longest test series boom is slightly longer than the longest DL6WU array.

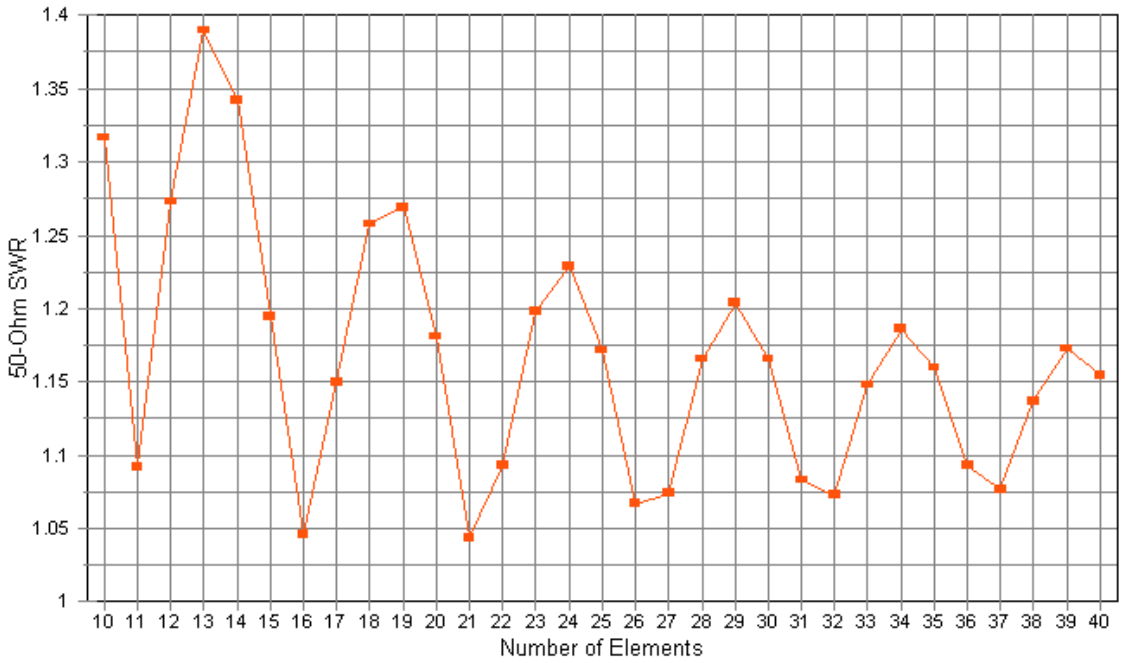
DL6WU 432-MHz Yagi Series: 40 Elements
50-Ohm SWR
50-Ohm SWR
1.4
1.35
1.3
1.25
1.2
1.15
1.1
1.05
1
10 11 12 13 14 15 16 17 18 19 20 21 22 23 24 25 26 27 28 29 30 31 32 33 34 35 36 37 38 39 40
Number of Elements

Fig. 13

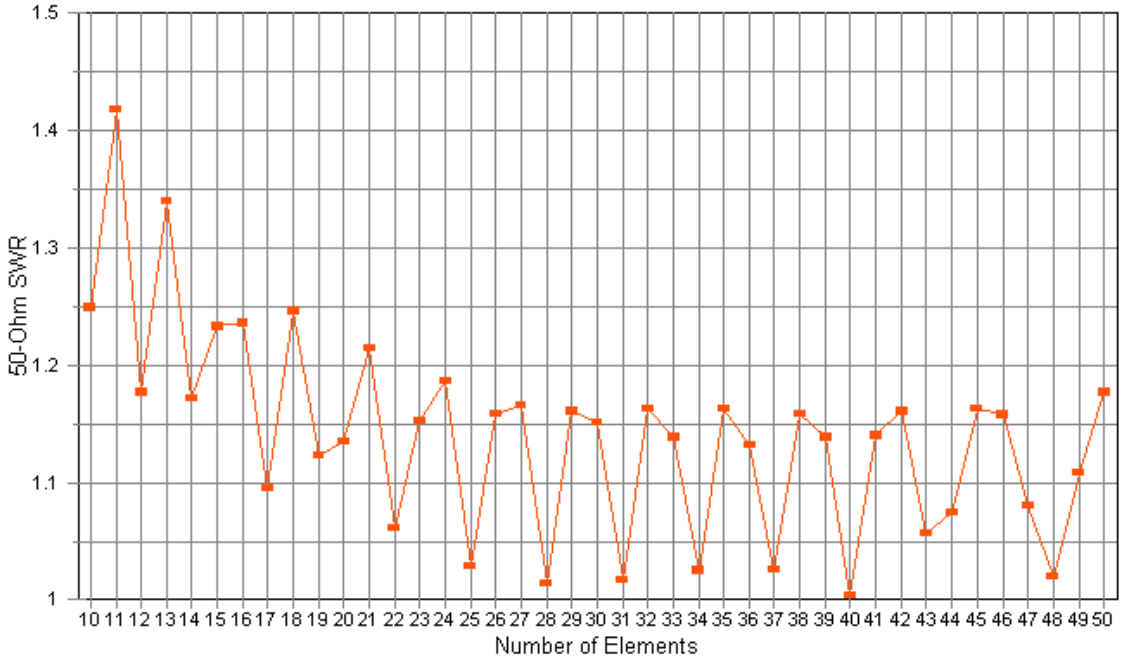
Test 432-MHz Yagi Series: 50 Elements
50-Ohm SWR
50-Ohm SWR
1.5
1.4
1.3
1.2
1.1
1
10 11 12 13 14 15 16 17 18 19 20 21 22 23 24 25 26 27 28 29 30 31 32 33 34 35 36 37 38 39 40 41 42 43 44 45 46 47 48 49 50
Number of Elements

Fig. 14

The SWR curves show reasonable values at 432 MHz for any length of either array. The shortest versions of each series show the widest SWR swings from one length to another. The key difference in the behavior of the 2 series of Yagis lies in the number of new elements between either SWR peaks or SWR dips. These values reflect the resistance and reactance behaviors of the arrays. The DL6WU arrays show a nearly uniform spacing of about 5 new elements between either peaks or dips. In contrast, the test series shows an average of about 3 new elements between peaks or dips, with the number increasing from about 2 new elements for short-boom versions to about 4 new elements for the greatest boomlengths. All of the questions applicable to the resistance and reactance behavior also apply to the behavior of the SWR curves.

The SWR curves complete the graphing of elements of the single-unit performance of the arrays at the design frequency. Since each version of each series of trimming Yagis is itself a wide-band antenna, we may be able to glean further interesting performance curves by examining frequency sweeps of them.

Wide-Band Performance from 400 to 460 MHz

Since the 2 Yagi series that we are exploring are inherently wide-band antennas, it is necessary to examine their performance--at least in a limited way--across their operating passband. That passband extends in all cases beyond the limits of the 70-cm amateur band (420-450 MHz). I cut off the limits for the frequency sweep at 400 MHz on the low end and 460 MHz on the upper end. The greater extension below the design frequency than above it is due to the standard Yagi characteristic of having the performance level fall off more slowly below the design frequency than above it. The free-space frequency sweeps used 1 MHz increments. For some parameters, a less sensitive increment would have sufficed, but to the degree possible, I wanted to be able to determine with relative non-ambiguity the frequency of SWR dips, front-to-back peaks, and peak gain. Even with a 1-MHz increment, a few ambiguous peaks remain, although their presence does not jeopardize the overall data.

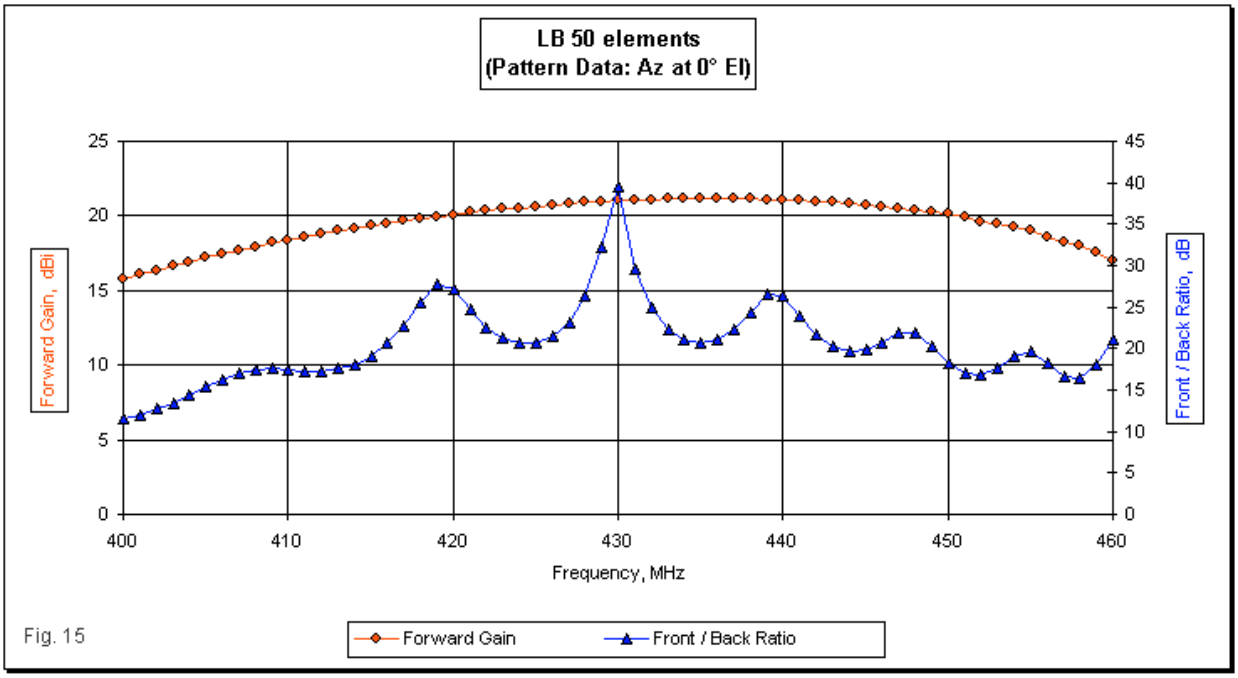

Fig. 15

The sweeps yielded EZ-Plots graphs for the gain and front-to-back ratio and for the resistance, reactance, and 50-Ohm SWR. **Fig. 15** and **Fig. 16** provide samples of the plots for one of the 72 runs. The full set of plots appears in the second part of this document.

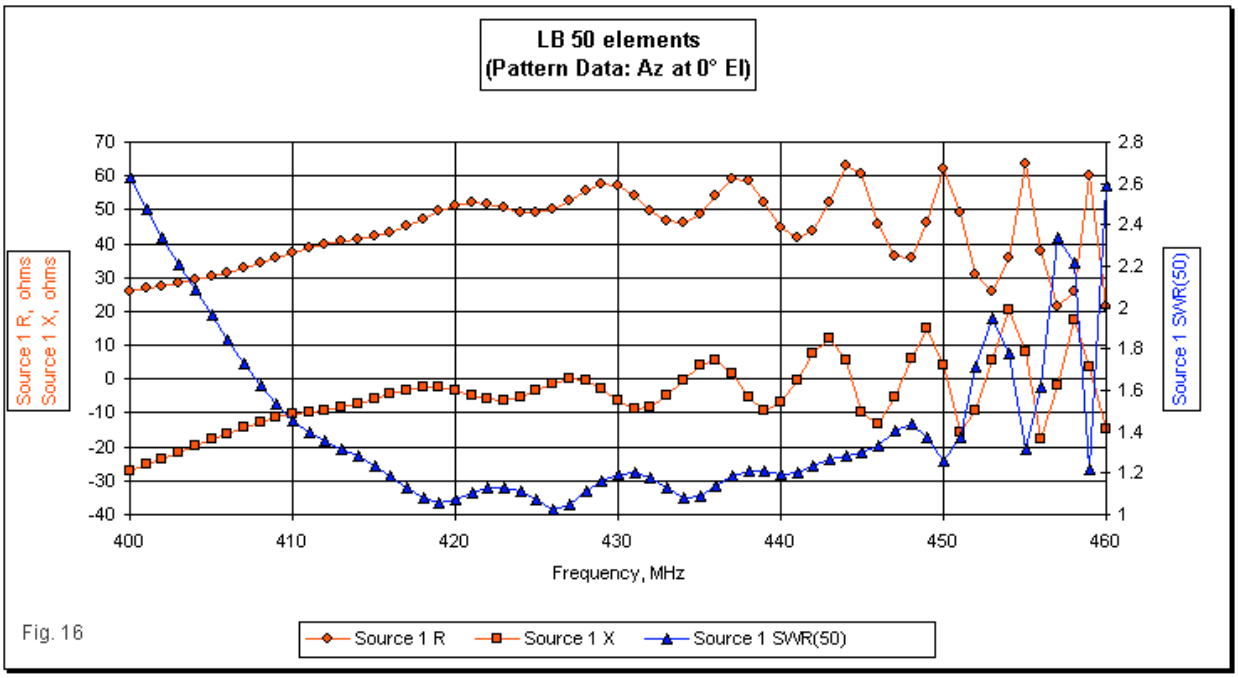

Fig. 16

For this discussion, we may divide the overall collection of data into 3 groupings:

1. Gain-related information;
2. Front-to-back ratio information; and
3. SWR information.

Gain-related data provides two important checks on performance of each Yagi within each series. The first check is on the usable gain vs. frequency of the individual arrays. The second check is on the uniformity or diversity of the difference between certain gain values, such as the design-frequency gain vs. the peak gain of which the array is capable.

The front-to-back data offers the possibility of seeing--at least in a limited way--the behavior of the 180° ratio as we move from one Yagi in a series to the next. The front-to-back ratio peaks show an odd set of behaviors when graphed at the design frequency across the span of boomlengths. The question at hand is whether the frequency-sweep data can shed any light on the patterns.

The SWR data will serve as a touchstone for all of the feedpoint information, since we have already seen that the SWR exhibits the same patterns as the resistance and reactance. As well, those patterns appear to have a relationship to the front-to-back patterns. Hence, a closer look at the SWR information is a first step toward a better understanding of trimming Yagi behavior in areas of relatively low design control.

1. *Gain-related information*: The key elements of gain date from each sweep include the frequency and the level of peak gain for each Yagi in each series. The difference between the frequency of peak gain and the design frequency may yield useful information. As well, the gain

values at both 420 and 450 MHz have some importance, since the Yagis are intended for use throughout that band. From the basic information, we can derive such figures as the total range of gain values within the band. Finally, we may note the gain values at the limits of the sweep as a measure of how slowly or rapidly performance falls off outside the range of intended use.

Table 7 provides in tabular form the gain-related information from the DL6WU series of Yagis.

Wide-Band Performance: WU10-WU40 Yagi Series											Table 7
Gain											
Elements	Bm-Ln	Gain 432	Pk Gn Fq	PkF-432	Pk Gain	PG-G432	Gn 420	Gn 450	Delta Gn	Gn 400	Gn 460
10	2.145068	13.88	437	5	14.04	0.16	13.11	13.27	0.93	10.77	11.52
11	2.490042	14.26	439.5	7.5	14.54	0.28	13.68	13.58	0.96	11.12	12.1
12	2.850003	14.76	441.5	9.5	14.95	0.19	14.1	13.9	1.05	11.47	12.46
13	3.224951	15.28	436	4	15.33	0.05	14.38	14.35	0.98	11.74	12.67
14	3.615028	15.69	436	4	15.82	0.13	14.72	14.88	1.1	11.98	12.74
15	4.015049	15.99	437.5	5.5	16.25	0.26	15.1	15.41	1.15	12.23	12.61
16	4.41507	16.27	438.5	6.5	16.62	0.35	15.42	15.84	1.2	12.45	12.29
17	4.814946	16.59	440	8	16.93	0.34	15.64	16.16	1.29	12.63	11.82
18	5.214967	16.92	441	9	17.19	0.27	15.83	16.36	1.36	12.8	11.31
19	5.614988	17.21	440.5	8.5	17.41	0.2	16.07	16.54	1.34	12.97	10.91
20	6.015008	17.43	437.5	5.5	17.69	0.26	16.32	16.77	1.37	13.13	10.83
21	6.415029	17.61	438	6	17.98	0.37	16.52	17.06	1.46	13.26	11.26
22	6.81505	17.82	439	7	18.23	0.41	16.66	17.38	1.57	13.39	12.2
23	7.215071	18.06	440	8	18.44	0.38	16.82	17.67	1.62	13.52	13.37
24	7.614947	18.28	441	9	18.62	0.34	17.01	17.88	1.61	13.64	14.33
25	8.014968	18.45	441	9	18.78	0.33	17.18	18.03	1.6	13.74	14.68
26	8.414989	18.59	438.5	6.5	18.97	0.38	17.31	18.18	1.66	13.85	14.41
27	8.815009	18.74	439	7	19.19	0.45	17.43	18.36	1.76	13.95	13.9
28	9.21503	18.92	440	8	19.37	0.45	17.56	18.58	1.81	14.05	13.56
29	9.61505	19.09	440.5	8.5	19.53	0.44	17.71	18.82	1.82	14.13	13.63
30	10.01507	19.23	441.5	9.5	19.67	0.44	17.84	19.02	1.83	14.22	14.15
31	10.41495	19.35	442	10	19.8	0.45	17.93	19.16	1.87	14.31	14.96
32	10.81497	19.47	439.5	7.5	19.95	0.48	18.03	19.28	1.92	14.39	15.78
33	11.21499	19.61	440	8	20.12	0.51	18.15	19.41	1.97	14.46	16.23
34	11.61501	19.75	440	8	20.27	0.52	18.27	19.57	2	14.53	16.18
35	12.01503	19.87	441	9	20.4	0.53	18.36	19.76	2.04	14.6	15.85
36	12.41505	19.97	442	10	20.51	0.54	18.44	19.93	2.07	14.67	15.6
37	12.81507	20.07	442	10	20.61	0.54	18.53	20.07	2.08	14.73	15.67
38	13.21495	20.18	440	8	20.74	0.56	18.63	20.18	2.11	14.8	16.09
39	13.61497	20.3	440	8	20.88	0.58	18.72	20.28	2.16	14.86	16.71
40	14.01499	20.4	441	9	21	0.6	18.79	20.4	2.21	14.92	17.28

Notes:											
Bm-Ln = Boom length in wavelengths						PG-G432 = Difference of gain at Pk Gn Fq and 432 MHz					
Gain 432 = Free-Space Gain at 432 MHz in dBi						Gn 420 = Gain at 420 MHz					
Pk Gn Fq = Peak gain frequency in MHz						Gn 450 = Gain at 450 MHz					
PkF-432 = Difference in peak gain and design frequencies						Delta Gn = Gain range within 70-cm amateur band					
Pk Gain = Gain at Pk Gn Fq						Gn 400 = Gain at 400 MHz					
						Gn 460 = Gain at 460 MHz					

The notes at the bottom of the table identify the columnar entries. Perhaps only the peak gain frequency values require explanation. In numerous cases, the same peak value appears at 2 or more contiguous frequencies. In such cases, the listed frequency is the arithmetic average of those frequencies. There was no simply way to indicate whether integer entries mean a single frequency peak or the average of 3 frequencies. However, the supplemental graphs for each sweep will clarify that question, should it prove important to any use of this data.

The equivalent information for the test series of Yagis appears in **Table 8**. The same explanation of the peak gain frequency applies to the values in this table. We shall follow the procedure so far used of comparing each graphed sub-category of data for the two series before changing to another sub-category.

Wide-Band Performance: LB10 to LB50 Yagi Series											Table 8
Gain Elements	Bm-Ln	Gain 432	Pk Gn Fq	PkF-432	Pk Gain	PG-G432	Gn 420	Gn 450	Delta Gn	Gn 400	Gn 460
10	1.52962	12.7	434.5	2.5	12.71	0.01	12.44	11.42	1.29	9.48	9.96
11	1.77685	13.28	430	-2	13.29	0.01	12.89	11.78	1.51	10.11	10.81
12	2.02258	13.64	433	1	13.64	0	13.35	12.25	1.39	10.31	11.22
13	2.28	14.08	429.5	-2.5	14.11	0.03	13.74	12.5	1.61	10.8	11.6
14	2.54783	14.46	432.5	0.5	14.46	0	14.09	13.03	1.43	10.99	12.16
15	2.82488	14.79	429.5	-2.5	14.81	0.02	14.47	13.37	1.44	11.39	12.59
16	3.11004	15.18	431.5	-0.5	15.18	0	14.73	13.72	1.46	11.54	12.92
17	3.40226	15.45	432.5	0.5	15.45	0	15.09	14.21	1.24	11.88	13.35
18	3.70057	15.78	430.5	-1.5	15.79	0.01	15.31	14.49	1.3	12.03	13.78
19	4.00408	16.08	432.5	0.5	16.08	0	15.6	14.83	1.25	12.29	14.05
20	4.31197	16.32	432.5	0.5	16.32	0	15.85	15.25	1.07	12.47	14.34
21	4.6235	16.61	432	0	16.61	0	16.06	15.5	1.11	12.63	14.73
22	4.93798	16.85	433.5	1.5	16.86	0.01	16.31	15.78	1.08	12.85	15
23	5.25483	17.07	433.5	1.5	17.07	0	16.49	16.14	0.93	12.96	15.17
24	5.57352	17.32	433	1	17.33	0.01	16.7	16.37	0.96	13.16	15.44
25	5.89361	17.52	434	2	17.55	0.03	16.91	16.58	0.97	13.28	15.73
26	6.21472	17.72	434.5	2.5	17.73	0.01	17.06	16.89	0.84	13.43	15.86
27	6.53657	17.94	433.5	1.5	17.95	0.01	17.26	17.11	0.84	13.59	15.97
28	6.85891	18.11	434.5	2.5	18.15	0.04	17.43	17.26	0.89	13.68	16.21
29	7.1816	18.29	435.5	3.5	18.32	0.03	17.57	17.5	0.82	13.84	16.39
30	7.50457	18.49	433.5	1.5	18.51	0.02	17.75	17.72	0.79	13.94	16.4
31	7.82782	18.64	435	3	18.69	0.05	17.89	17.84	0.85	14.06	16.49
32	8.15142	18.81	435.5	3.5	18.84	0.03	18.03	18.01	0.83	14.19	16.68
33	8.47553	18.98	434	2	19.01	0.03	18.19	18.22	0.82	14.27	16.73
34	8.80036	19.11	435.5	3.5	19.17	0.06	18.31	18.32	0.86	14.4	16.68
35	9.12621	19.26	436	4	19.3	0.04	18.45	18.43	0.87	14.49	16.76
36	9.45346	19.42	434	2	19.45	0.03	18.59	18.61	0.86	14.59	16.88
37	9.78155	19.54	435	3	19.61	0.07	18.7	18.73	0.91	14.7	16.83
38	10.114	19.68	436.5	4.5	19.73	0.05	18.83	18.79	0.94	14.77	16.76
39	10.4484	19.83	434.5	2.5	19.86	0.03	18.96	18.92	0.94	14.88	16.83
40	10.7865	19.94	435.5	3.5	20	0.06	19.05	19.07	0.95	14.97	16.91
41	11.1289	20.06	436	4	20.12	0.06	19.18	19.14	0.98	15.04	16.85
42	11.4766	20.2	435	3	20.23	0.03	19.3	19.2	1.03	15.14	16.77
43	11.8303	20.32	434.5	2.5	20.37	0.05	19.39	19.33	1.04	15.22	16.8
44	12.1911	20.42	435.5	3.5	20.49	0.07	19.5	19.47	1.02	15.28	16.9
45	12.56	20.54	436.5	4.5	20.6	0.06	19.61	19.55	1.05	15.38	16.96
46	12.9381	20.67	435.5	3.5	20.7	0.03	19.71	19.61	1.09	15.45	16.95
47	13.3266	20.78	434.5	2.5	20.83	0.05	19.79	19.69	1.14	15.51	16.91
48	13.7268	20.88	435	3	20.96	0.08	19.9	19.82	1.14	15.58	16.91
49	14.1401	20.99	435.5	3.5	21.08	0.09	20	19.97	1.11	15.67	16.95
50	14.5677	21.1	436	4	21.2	0.1	20.1	20.12	1.1	15.74	17
Notes:											
Bm-Ln = Boom length in wavelengths						Gn 420 = Gain at 420 MHz					
Gain 432 = Free-Space Gain at 432 MHz in dBi						Gn 450 = Gain at 450 MHz					
Pk Gn Fq = Peak gain frequency in MHz						Delta Gn = Gain range within 70-cm amateur band					
Pk Gain = Gain at Pk Gn Fq						Gn 400 = Gain at 400 MHz					
PG-G432 = Difference of gain at Pk Gn Fq and 432 MHz						Gn 460 = Gain at 460 MHz					

We may collect almost all of the raw gain values into a single graph for each series. **Fig. 17** shows the following gain values for the DL6WU series of arrays: gain at 400 MHz, gain at 420 MHz, gain at 432 MHz (the design frequency), peak gain (at whatever frequency it occurs), gain at 450 MHz, and gain at 460 MHz. Since the DL6WU series adhered to the antenna dimensions dictated by the program dl6wu-gg.exe, there is a very noticeable difference between the design-frequency gain and the peak gain. Interestingly, the gain at 450 MHz tends to track the peak gain, while the gain at 420 MHz tends to track the gain at the design frequency. Since performance falls off rapidly above the design passband, the gain at 460 MHz shows undulations, with 3 definite and a possible 4th peak within the overall frequency-sweep range. Because performance falls off slowly below the design passband, the curve for 400 MHz is smooth.

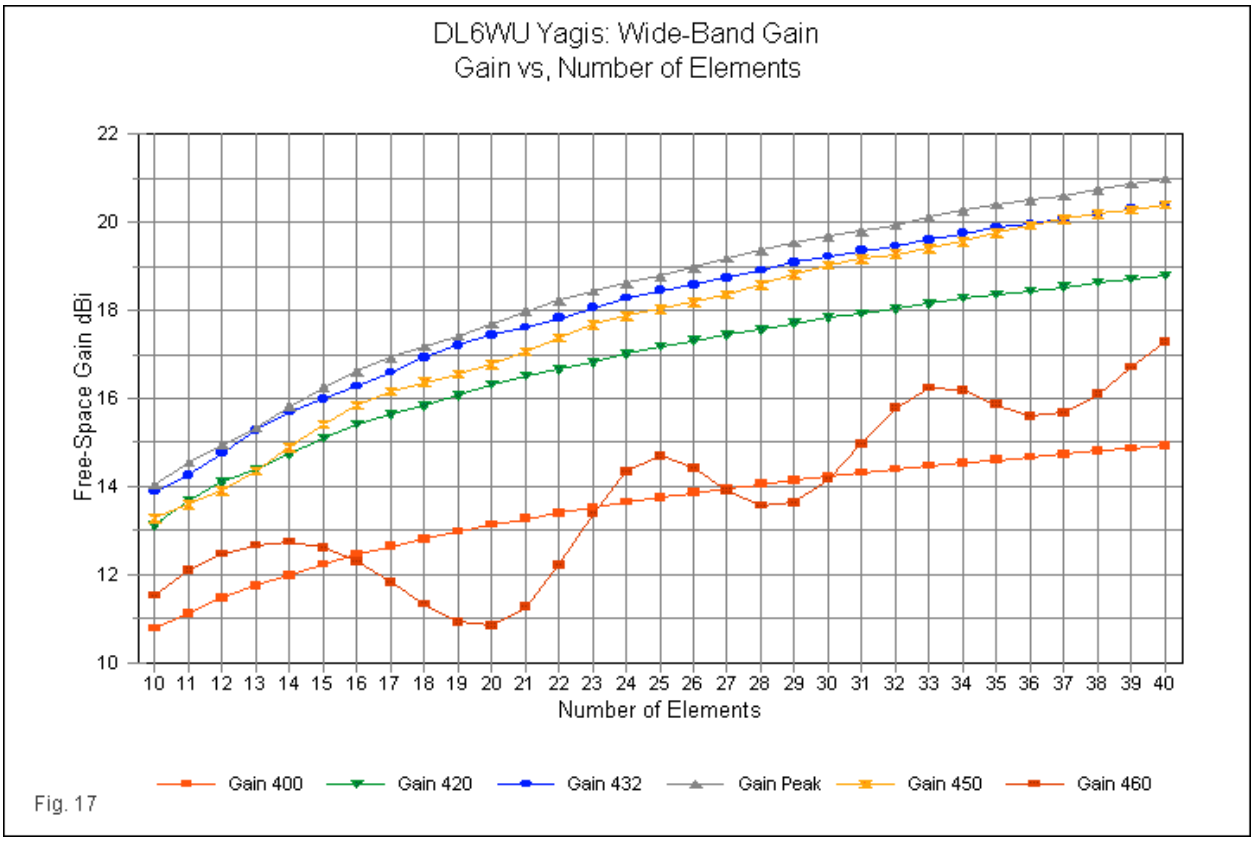
DL6WU Yagis: Wide-Band Gain
Gain vs, Number of Elements
Free-Space Gain dBi
22
20
18
16
14
12
10
10 11 12 13 14 15 16 17 18 19 20 21 22 23 24 25 26 27 28 29 30 31 32 33 34 35 36 37 38 39 40
Number of Elements
Gain 400
Gain 420
Gain 432
Gain Peak
Gain 450
Gain 460

Fig. 17

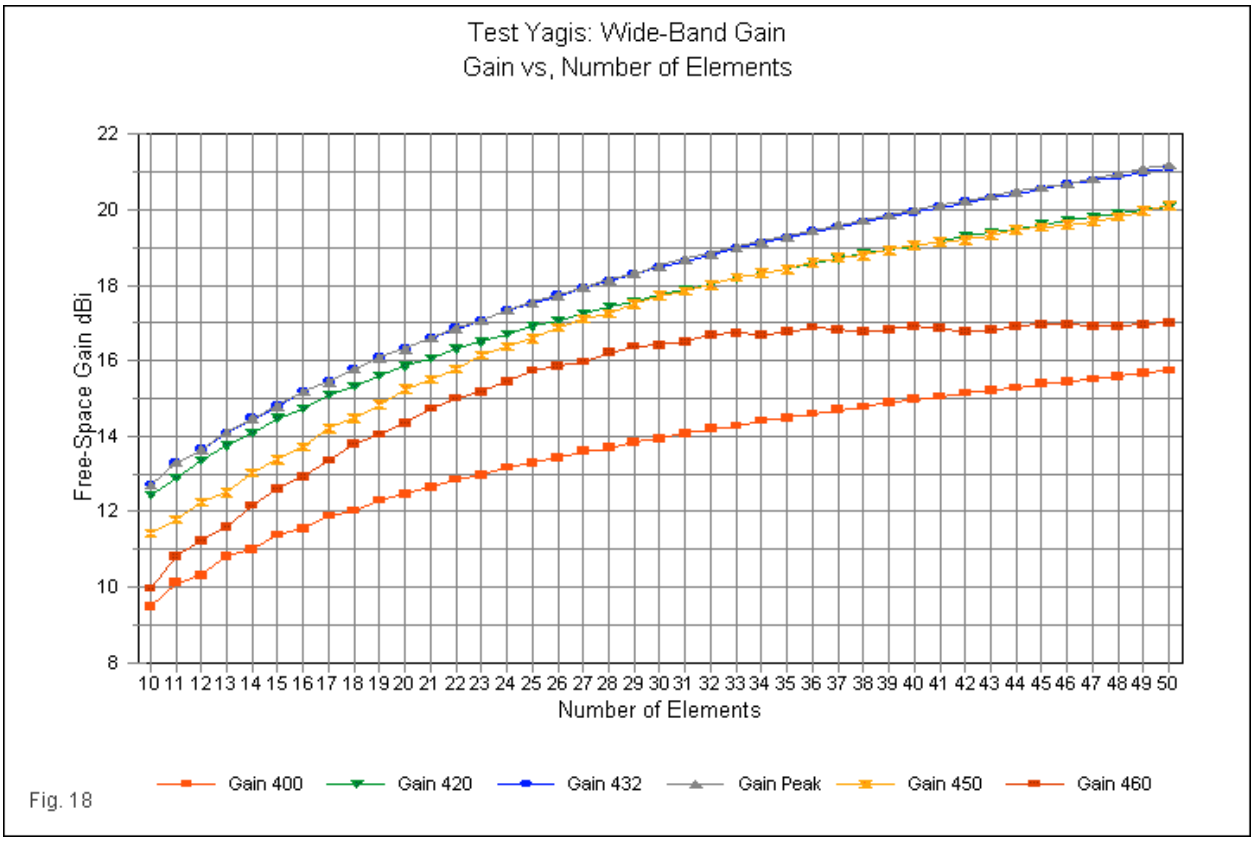
Test Yagis: Wide-Band Gain
Gain vs, Number of Elements
Free-Space Gain dBi
22
20
18
16
14
12
10
8
10 11 12 13 14 15 16 17 18 19 20 21 22 23 24 25 26 27 28 29 30 31 32 33 34 35 36 37 38 39 40 41 42 43 44 45 46 47 48 49 50
Number of Elements
Gain 400
Gain 420
Gain 432
Gain Peak
Gain 450
Gain 460

Fig. 18

The test series of Yagis intentionally brought the peak gain frequency and the design frequency together, although not perfectly. However, at the scale graphed in **Fig. 18**, the peak gain and the design-frequency gain values virtually overlay each other. For shorter boomlengths, the gain at 420 MHz exceeds the gain at 450 MHz. However, at mid-range (about 30 elements), the higher-frequency gain catches up to the lower-frequency value and the 2 values are very similar for all longer-boom versions of the test series Yagi.

The sweep limit curves are very similar in many ways to those for the DL6WU Yagis. At 400 MHz, the gain values show a smooth curve. At 460 MHz, the gain curve undulates as an indication of performance outside the design range. However, despite the lowering of the frequency of peak gain, the 460-MHz gain undulations are much shallower than those for the DL6WU array. In addition, separation as the arrays grow longer, the peaks in the ripple appear at a wider, possibly as a function of the increasing space between added directors. However, the number of peaks far exceeds those found with the DL6WU series. In this last phenomenon, we find echoes of the differences between the series with respect to both front-to-back ratio and feedpoint information.

An alternative way to examine the gain data is to pay close attention to certain differentials. Particularly significant at face value is the difference in frequency between the design frequency and the frequency of peak gain. For the moment, we shall note this difference and later see what it may (or may not) indicate. As well, at least two gain differentials are notable. One is the gain difference between the design frequency and the frequency of peak gain. The other is the range of gain within the 70-cm amateur band, the design passband for the antennas.

The DL6WU differentials appear in **Fig. 19**. The blue line references the right-hand Y-axis labels and indicates the frequency difference between the design frequency and the peak-gain frequency. The peak gain frequency varies from 436 to 442 MHz or 4 to 10 MHz above the design frequency. However, notice that the separation moves in nearly saw-tooth waves, with 5 distinct peaks across the span of array sizes explored here. The red line, with a left Y-axis reference, records the total range of gain values for each size array using 420 and 450 MHz as the limits. The gain range varies from about 0.9 dB for very short booms up to about 2.2 dB for very long booms. The green line, also with a left Y-axis reference, records the difference in gain between the value at 432 MHz and the peak gain. This value also increases with boomlength from about 0.2 dB up to 0.6 dB. It is interesting that the red and green lines end with relative smooth curves. However, for shorter boom lengths, they both show undulations that are almost in step with the amount of frequency separation between the design frequency and the maximum gain frequency.

The test-series differentials appear in **Fig. 20**. The blue line indicating the amount of frequency separation between the design frequency and the peak-gain frequency has a right axis scale that is less than half that for the DL6WU series. Hence, the wide changes of line length between points are far less significant than they may at first appear. More significant in all likelihood is the number of peaks in the series and the spacing between peaks. The spacing between peaks shows much the same growth from 2 elements to 4 elements as we increase the boomlength and increase the spacing between adjacent directors. The total gain differential across the 420-450-MHz span hovers around the 1-dB mark except for the shorter boomlengths. The increased differential for shorter booms corresponds to the lower gain shown in the 450-MHz line in **Fig. 18**. The gain differential between the design frequency and peak-gain frequency is very small and reaches 0.1 dB for only the longest boom in the series. The small undulations in both of these series of differentials is almost--but not quite--in step with the curve recording the frequency differential between peak gain and the design frequency.

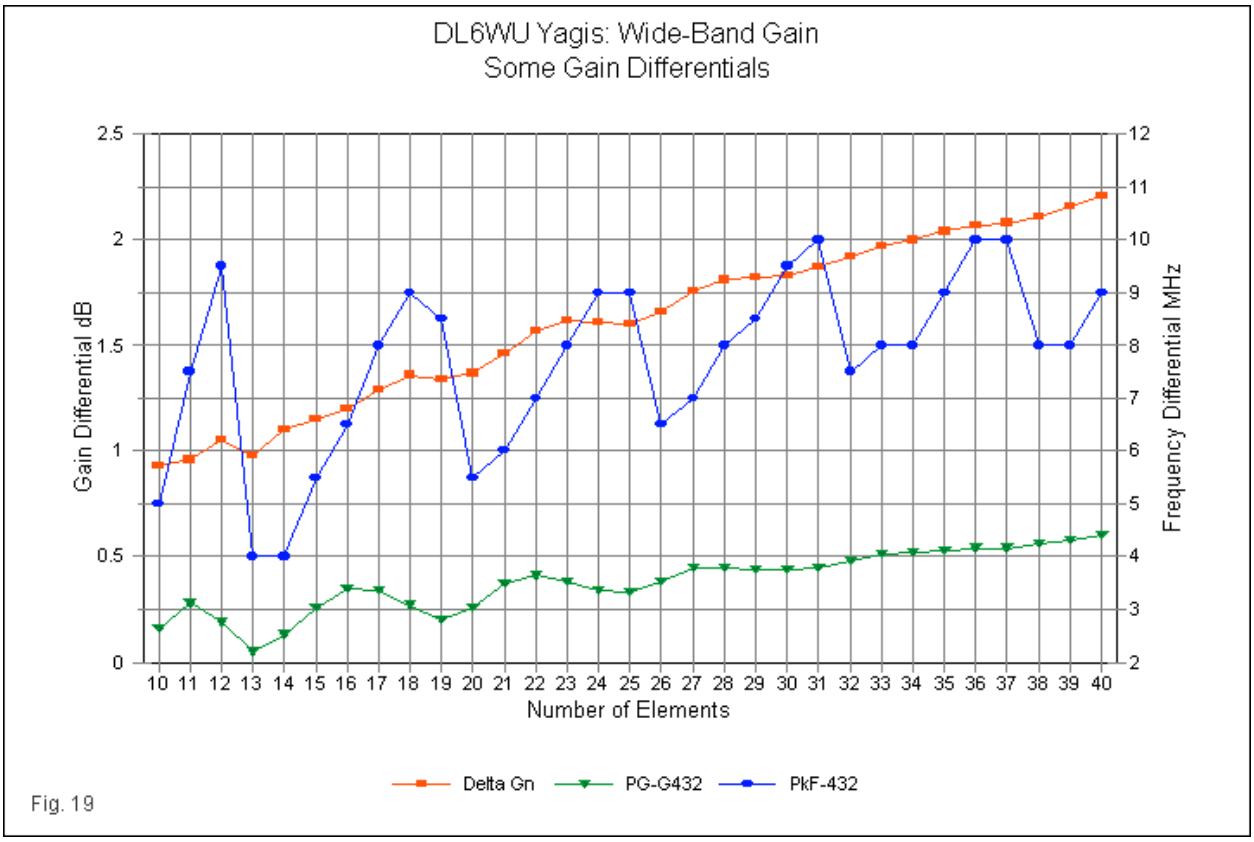
DL6WU Yagis: Wide-Band Gain
Some Gain Differentials
Gain Differential dB
Frequency Differential MHz
Number of Elements
Delta Gn
PG-G432
PkF-432

Fig. 19

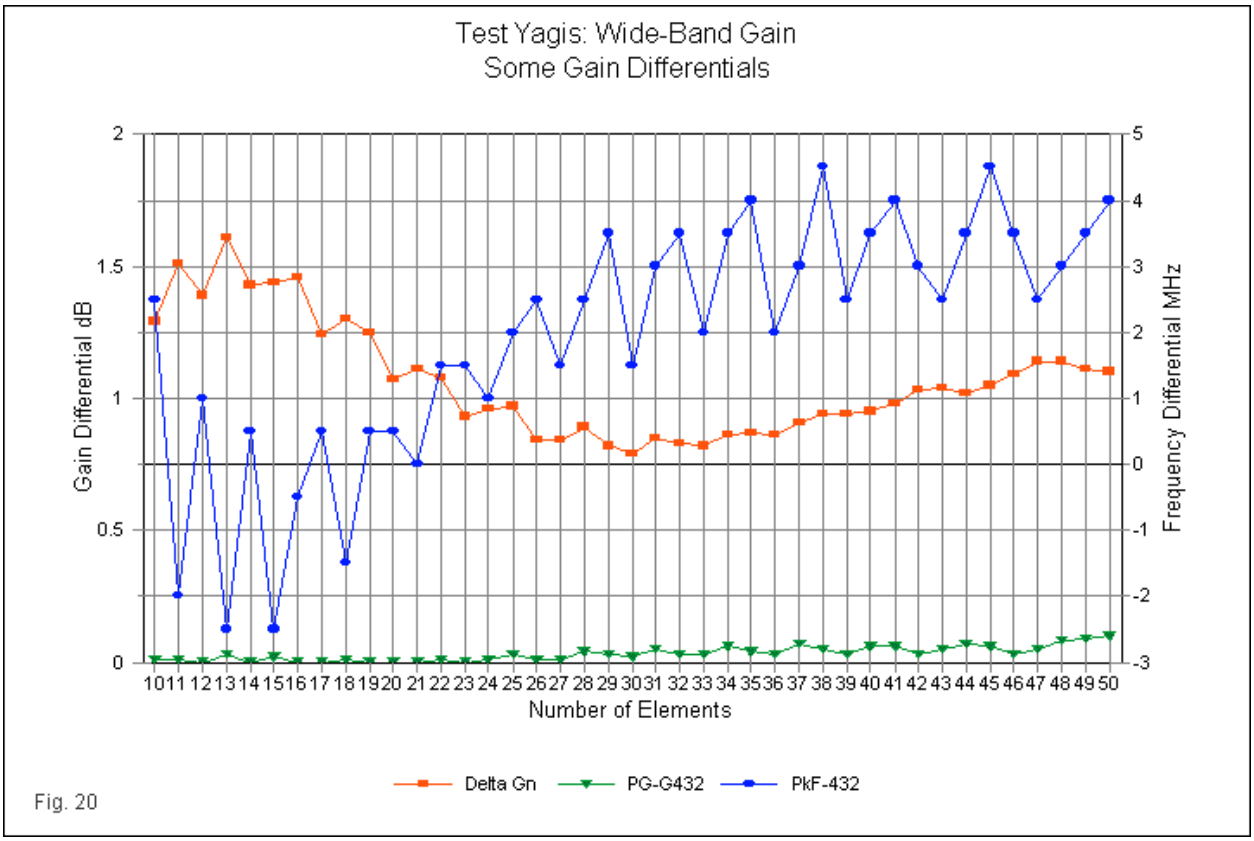
Test Yagis: Wide-Band Gain
Some Gain Differentials
Gain Differential dB
Frequency Differential MHz
Number of Elements
Delta Gn
PG-G432
PkF-432

Fig. 20

As we noted earlier, there are indications in the data that the beamwidth is not solely a function of gain, but may also involve the strength of the forward-most sidelobes. The stronger the sidelobes--or the smaller the front-to-sidelobe ratio--the narrower the beamwidth of the main forward lobe. There is a second possible trend related to this one. Virtually all designs with weaker forward sidelobes--or higher front-to-sidelobe ratio values--appear to have a wider separation between the design frequency and the frequency of maximum gain, with the latter being higher in frequency. As a result, such designs tend to have lower design-frequency gain values than Yagis of equivalent boomlengths but designed almost solely for maximum gain. Review **Table 3** for samples, understanding that samples may be suggestive but do not prove a general case.

2. *Front-to-back ratio information*: There are numerous aspects of the wide-band data for the front-to-back ratios of the 2 Yagis series that deserve attention. In these notes, we shall deal with only two facets of this relatively uncontrolled characteristic of the trimming Yagis. The first feature is the variability of 180° front-to-back values across the swept passband, with stops at 400, 420, 432, 450, and 460 MHz.

The data for the DL6WU series appears in **Table 9**. Corresponding data for the test series is in **Table 10**. In both cases, we find a morass of information that almost seems to defy systematic treatment. However, if we graph some of the information, some useful patterns begin to emerge. For example, **Fig. 21** shows the curves created by the data for the DL6WU series of Yagis. The lower curves represent the front-to-back ratio at the edges of the sweep range: 400 and 460 MHz. Note that for the DL6WU series, both sets of front-to-back ratio values are very significantly lower than the values for the edges and near-center of the 70-cm amateur band. We can distinguish the design-frequency (blue) line by the sharply higher peak values reached. In fact, below about 425 MHz and above 455 MHz, front-to-back peak values rarely reach higher than about 25 dB. Values above 30 dB remain almost exclusively in the 430-440-MHz range.

The values for each frequency in the set of curves describe cycles of higher and lower values. Interestingly, the higher the frequency, the fewer the number of cycles over the 10 to 40 elements of Yagi length.

400 MHz	8 cycles
420 MHz	7 cycles
432 MHz	7 cycles
450 MHz	5 cycles
460 MHz	4 cycles

The number of cycles diminishes by half with increasing frequency, although the frequency range is only about 14% of the center frequency within it. Obviously, more is at work in determining the number of cycles of front-to-back ratio excursion than a simple combination of boomlength, number of elements, and frequency change.

Table 9 also records the number of peak front-to-back values encountered for each Yagi length, expressed in terms of the number of elements. We shall examine those peaks shortly. For the present, we may note that to pack more peaks into a given passband, the lowest value of front-to-back ratio reached between the peaks is a higher value than when there are few peaks. As a result, the longer the DL6WU Yagi, the less chance there is in encountering a front-to-back ratio under 20 dB anywhere within the 70-cm amateur band.

Wide-Band Performance: WU10-WU40 Yagi Series							Table 9
Front-to-Back Ratio							
Elements	Bm-Ln	180 F-B	FB 400	FB 420	FB 450	FB 460	# Peaks
10	2.145068	31.92	7.11	14.62	15.37	14.45	2
11	2.490042	16.96	8.89	14.86	14.15	17.32	3
12	2.850003	15.49	7.72	23.17	16.6	15.85	3
13	3.224951	19.31	8.02	18.91	21.68	12.69	2
14	3.615028	28.63	9.58	15.12	21.38	10.36	2
15	4.015049	21.14	9.41	15.81	17.58	8.68	3
16	4.41507	17.54	8.61	20.79	15.84	7.62	3
17	4.814946	17.68	9.24	23.82	15.95	7.11	3
18	5.214967	21.43	10.33	18	17.92	7.22	3
19	5.614988	33.2	9.89	16.63	22.58	8.11	4
20	6.015008	24.37	9.38	18.98	27.88	10.06	4
21	6.415029	19.8	10.08	24.53	22.2	13.08	4
22	6.81505	19.51	10.82	21.34	18.79	15	4
23	7.215071	22.92	10.29	18.06	17.9	13.63	5
24	7.614947	35.99	9.99	18.45	19.08	12.03	4
25	8.014968	26.69	10.7	22.29	22.81	11.45	4
26	8.414989	21.48	11.17	24.33	29.97	11.99	4
27	8.815009	20.94	10.61	20.09	25.61	13.63	4
28	9.21503	24.14	10.5	18.76	21	15.88	5
29	9.61505	37.43	11.18	20.7	19.48	16.27	5
30	10.01507	28.42	11.42	24.73	20.16	14.37	4
31	10.41495	22.83	10.91	22.54	23.32	12.78	4
32	10.81497	22.14	10.94	19.76	30.62	12.33	5
33	11.21499	25.2	11.58	20.05	28.48	13.07	5
34	11.61501	38.02	11.63	23.19	22.84	15.18	5
35	12.01503	29.7	11.16	24.64	20.83	18.56	4
36	12.41505	23.93	11.31	21.34	21.16	19.51	6
37	12.81507	23.15	11.87	20.17	23.95	16.35	5
38	13.21495	26.12	11.8	21.84	31.02	14.02	5
39	13.61497	38.19	11.41	24.96	31.08	13.18	5
40	14.01499	30.61	11.65	23.27	24.42	13.74	6
Notes:	Bm-Ln = Boom length in wavelengths						
	180 F-B = 180-degree front-to-back ratio at 432 MHz						
	FB 400 = 180-degree front-to-back ratio at 400 MHz						
	FB 420 = 180-degree front-to-back ratio at 420 MHz						
	FB 450 = 180-degree front-to-back ratio at 450 MHz						
	FB 460 = 180-degree front-to-back ratio at 460 MHz						
	# Peaks = Number of F-B peaks from 400 to 460 MHz						

The data for the test series of Yagis with 10 to 50 elements tells a similar story, but with some significant differences. For example, the number of cycles for each frequency rises dramatically, but shows the same set of trends. See **Fig. 22** for the complete test-series Yagi front-to-back data.

400 MHz 15 cycles
420 MHz 15 cycles
432 MHz 14 cycles
450 MHz 12 cycles
460 MHz 12 cycles

Wide-Band Performance: LB10 to LB50 Yagi Series							Table 10
Front-to-Back Ratio							
Elements	Bm-Ln	180 F-B	FB 400	FB 420	FB 450	FB 460	# Peaks
10	1.52962	17.6	5.81	12.25	15.11	19.58	1
11	1.77685	16.96	5.97	21.28	28.69	14.15	2
12	2.02258	19.6	7.16	13.37	16.82	25.95	2
13	2.28	17.04	6.52	21.67	26.78	15.16	2
14	2.54783	25.31	7.84	14.35	19.5	17.08	2
15	2.82488	16.19	7.25	21	20.8	23.12	3
16	3.11004	34.39	8.13	15.81	27.57	15.66	2
17	3.40226	18.46	8.08	18.37	19.19	19.18	3
18	3.70057	21.34	8.19	18.93	25.73	23.55	3
19	4.00408	25.33	8.97	16.52	23.97	16.72	2
20	4.31197	18.76	8.26	22.72	19.84	19.04	3
21	4.6235	28.14	9.57	17.09	27.29	26.54	3
22	4.93798	22.1	8.67	19.47	24.06	18.22	3
23	5.25483	20.12	9.55	20.97	20.16	18.14	3
24	5.57352	36.5	9.49	17.44	25.98	25.84	3
25	5.89361	21.34	9.28	22.63	25.45	20.96	3
26	6.21472	21.56	10.26	19.35	20.37	17.86	3
27	6.53657	37.54	9.42	18.71	24.1	21.63	4
28	6.85891	21.18	10.32	24.01	27.54	25.6	4
29	7.1816	22.97	10.11	18.69	20.76	18.85	3
30	7.50457	33.15	9.99	20.61	22.55	19.18	4
31	7.82782	21.23	10.84	22.99	29.19	26.46	4
32	8.15142	24.43	10.04	18.74	21.49	21.57	4
33	8.47553	30.48	10.9	22.95	21.45	18.52	4
34	8.80036	21.4	10.68	21.53	28.48	21.97	4
35	9.12621	25.69	10.53	19.36	22.77	26.74	5
36	9.45346	29.4	11.37	24.92	20.76	19.72	4
37	9.78155	21.68	10.6	20.7	25.68	19.39	4
38	10.114	26.02	11.27	20.18	25.15	25.44	5
39	10.4484	30.71	11.35	25.7	20.78	24.54	5
40	10.7865	22.09	10.88	20.64	22.4	19.53	5
41	11.1289	24.66	11.77	20.6	27.77	20.1	5
42	11.4766	40.83	11.37	26.04	22.85	26.07	5
43	11.8303	23.57	11.21	21.57	20.56	26.52	6
44	12.1911	22.45	12.03	20.22	22.22	20.75	5
45	12.56	28.54	11.67	24.24	26.13	19.35	5
46	12.9381	34.4	11.34	25.42	24.12	20.59	6
47	13.3266	23.92	12.03	20.99	20.7	23.89	6
48	13.7268	21.71	12.34	20.22	19.13	27.05	6
49	14.1401	22.34	11.81	22.35	18.6	24.64	6
50	14.5677	24.84	11.53	27.12	18.26	21.1	7
Notes:	Bm-Ln = Boom length in wavelengths						
	180 F-B = 180-degree front-to-back ratio at 432 MHz						
	FB 400 = 180-degree front-to-back ratio at 400 MHz						
	FB 420 = 180-degree front-to-back ratio at 420 MHz						
	FB 450 = 180-degree front-to-back ratio at 450 MHz						
	FB 460 = 180-degree front-to-back ratio at 460 MHz						
	# Peaks = Number of F-B peaks from 400 to 460 MHz						

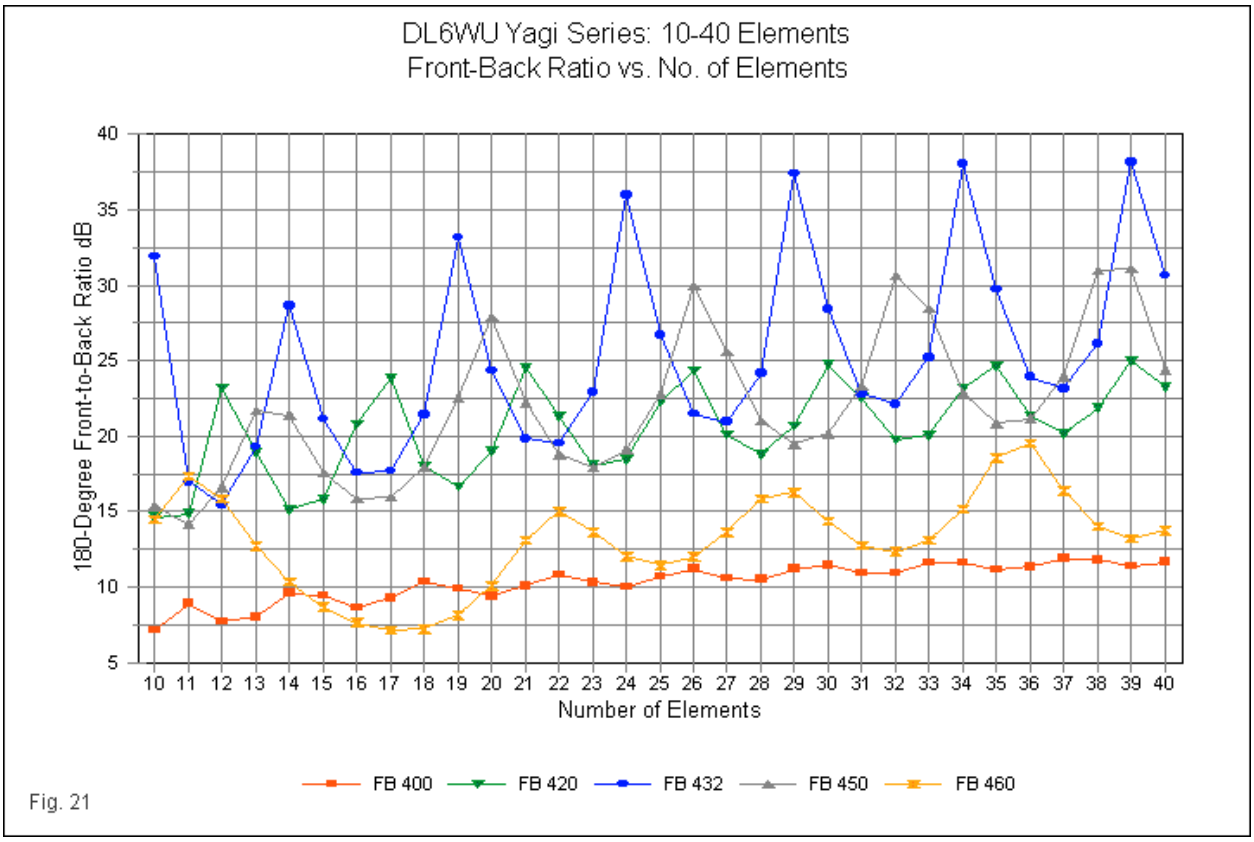
DL6WU Yagi Series: 10-40 Elements
Front-Back Ratio vs. No. of Elements
180-Degree Front-to-Back Ratio dB
Number of Elements
FB 400
FB 420
FB 432
FB 450
FB 460

Fig. 21

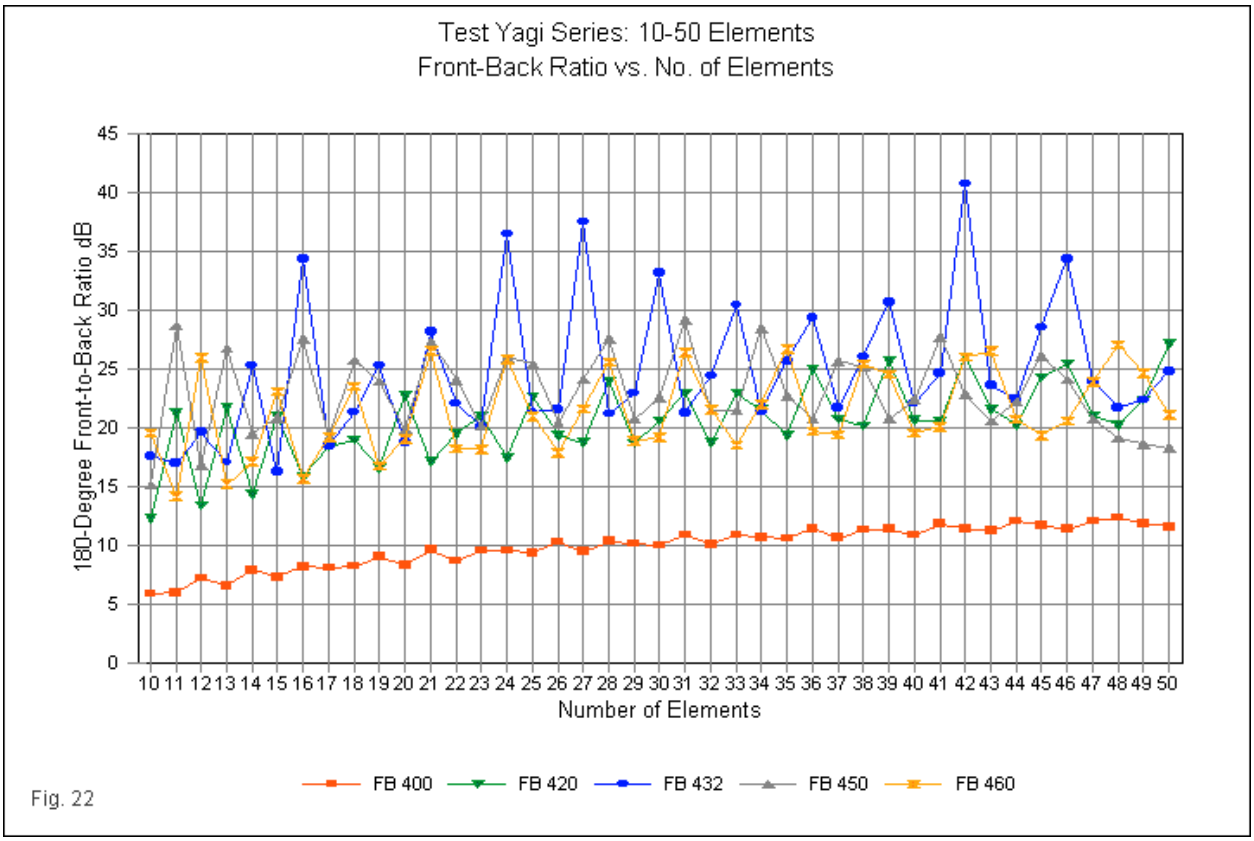
Test Yagi Series: 10-50 Elements
Front-Back Ratio vs. No. of Elements
180-Degree Front-to-Back Ratio dB
Number of Elements
FB 400
FB 420
FB 432
FB 450
FB 460

Fig. 22

A second way in which the test series data differ from the information for the DL6WU series is in the level of front-to-back ratio at 460 MHz. The test series values are so close to the data for 420 through 450 MHz as to make the lines almost unreadable in their crossing ways. The improved front-to-back performance at 460 MHz--whatever its utility--has a further consequence: it allows at least one additional peak within the overall swept passband. Whereas the DL6WU series showed a maximum of 6 peaks within the passband, the test series has a maximum of 7. Both series tend to restrict the very highest peak values for the 430-440-MHz region, with a gradual tapering of maximum values toward each end of the swept frequency range.

The nature of the peak values themselves holds some interest, since spot checks suggest that the peaks move in frequency with the addition of new directors. However, by skipping some Yagi lengths, spot checks tend to leave the movement ambiguous. Of course, we have already noted the increasing number of front-to-back peaks as we add elements, so we also know that the frequency spacing between peaks must compress as we increase the element count. To determine the movement and compression of front-to-back peaks, I recorded the peak frequencies. **Table 11** records the data for the DL6WU series. The test series of Yagis has the same data set in **Table 12**. The DL6WU series identifies only 10 moving peaks and hence is legible in normal form. However, for the test series of Yagis, there are 17 moving peaks. Hence, **Table 12** appears in normal but small form (for screen reading) and also in larger form tilted 90° (for paper reading). Both tables include in their data division an interpretation of the data in the association of peak frequencies with a peak number.

Wide-Band Performance: WU10-WU40 Yagi Series — Table 11

Front-to-Back Ratio Peaks and Frequencies

Elements	Bm-Ln	Peak 1	Peak 2	Peak 3	Peak 4	Peak 5	Peak 6	Peak 7	Peak 8	Peak 9	Peak 10
10	2.145068	456	432								
11	2.490042	458	439	416							
12	2.850003	455	445	420							
13	3.224951		449	426							
14	3.615028		452	431							
15	4.015049		453	435	414						
16	4.41507		454	438	418						
17	4.814946		455	441	423						
18	5.214967		456	444	427						
19	5.614988		457	447	431	413					
20	6.015008		458	450	434	416					
21	6.415029		458	452	437	420					
22	6.81505		459	453	440	424					
23	7.215071		459	454	442	428	413				
24	7.614947			455	445	431	415				
25	8.014968			456	447	434	418				
26	8.414989			457	449	436	422				
27	8.815009			457	451	439	425				
28	9.21503			458	453	441	428	414			
29	9.61505			458	454	443	431	417			
30	10.01507				455	445	434	420			
31	10.41495				455	447	436	423			
32	10.81497				456	449	438	426	413		
33	11.21499				457	451	440	429	416		
34	11.61501				457	452	442	431	419		
35	12.01503				458	453	444	434	422		
36	12.41505				458	454	446	436	424	413	
37	12.81507					456	448	437	427	415	
38	13.21495					456	449	439	429	418	
39	13.61497					456	451	441	431	420	
40	14.01499					457	452	443	433	423	413

Wide-Band Performance: LB10 to LB50 Yagi Series																		Table 12
Front-to-Back Ratio Peaks and Frequencies																		
Elements	Bm-Ln	Peak 1	Peak 2	Peak 3	Peak 4	Peak 5	Peak 6	Peak 7	Peak 8	Peak 9	Peak 10	Peak 11	Peak 12	Peak 13	Peak 14	Peak 15	Peak 16	Peak 17
10	1.52962	439																
11	1.77685	451	423															
12	2.02258	459	438															
13	2.28		448	423														
14	2.54783		456	435														
15	2.82488		460	445	421													
16	3.11004			452	431													
17	3.40226			457	440	418												
18	3.70057			460	447	427												
19	4.00408				453	435												
20	4.31197				457	442	422											
21	4.6235				460	448	430											
22	4.93798					453	437	418										
23	5.25483					456	443	425										
24	5.57352					459	448	432										
25	5.89361						452	438	420									
26	6.21472						455	443	426									
27	6.53657						458	447	433	416								
28	6.85891						460	451	438	421								
29	7.1816							454	443	428								
30	7.50457							457	447	433	417							
31	7.82782							460	450	438	423							
32	8.15142								453	442	429	414						
33	8.47553								456	446	434	419						
34	8.80036								458	449	438	424						
35	9.12621								460	452	442	429	415					
36	9.45346									455	446	434	420					
37	9.78155									457	449	438	425					
38	10.114									459	451	442	429	416				
39	10.4484									460	454	445	433	421				
40	10.7865										456	447	437	425	413			
41	11.1289										458	450	440	429	416			
42	11.4766										459	452	443	432	420			
43	11.8303										460	454	446	436	424	412		
44	12.1911											455	448	438	427	415		
45	12.56											457	449	441	430	419		
46	12.9381											458	451	443	433	422	411	
47	13.3266											459	452	444	435	424	413	
48	13.7268											460	453	446	437	427	415	
49	14.1401											460	454	447	438	428	418	
50	14.5677											460	455	448	439	430	419	410

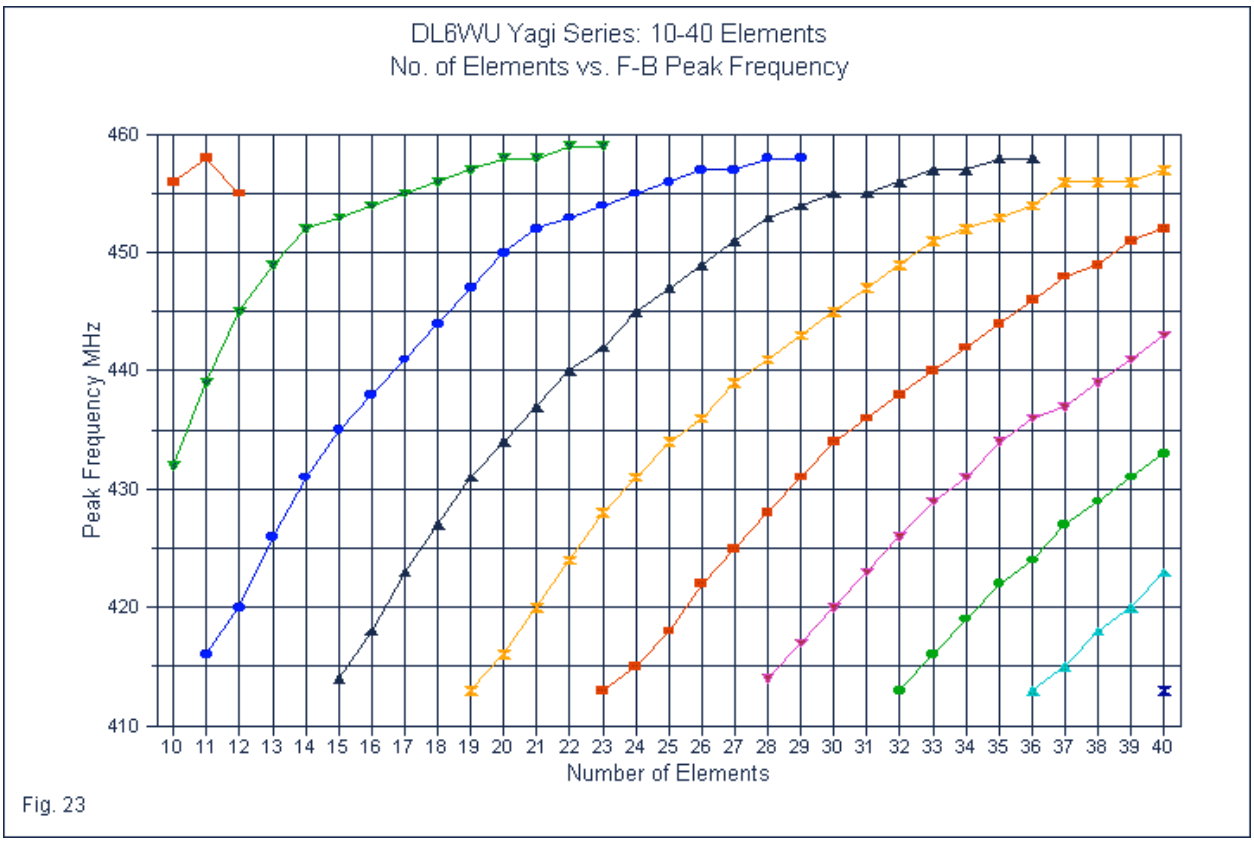

Fig. 23

Fig. 23 translates the data in **Table 11** into graphical form to show the apparent movement of each peak upward in frequency as we add new directors. The graph also shows the slowing rate of peak frequency increase as it approaches 460 MHz.

Wide-Band Performance: LB10 to LB50 Yagi Series — Table 12

Front-to-Back Ratio Peaks and Frequencies

Elements	Bm-Ln	Peak 1	Peak 2	Peak 3	Peak 4	Peak 5	Peak 6	Peak 7	Peak 8	Peak 9	Peak 10	Peak 11	Peak 12	Peak 13	Peak 14	Peak 15	Peak 16	Peak 17
10	1.52962	439																
11	1.77685	451	423															
12	2.02258	459	438															
13	2.28		448	423														
14	2.54783		456	435														
15	2.82488		460	445	421													
16	3.11004			452	431													
17	3.40226			457	440	418												
18	3.70057			460	447	427												
19	4.00408				453	435												
20	4.31197				457	442	422											
21	4.6235				460	448	430											
22	4.93798					453	437	418										
23	5.25483					456	443	425										
24	5.57352					459	448	432										
25	5.89361						452	438	420									
26	6.21472						455	443	426									
27	6.53657						458	447	433	416								
28	6.85891						460	451	438	421								
29	7.1816							454	443	428								
30	7.50457							457	447	433	417							
31	7.82782							460	450	438	423							
32	8.15142								453	442	429	414						
33	8.47553								456	446	434	419						
34	8.80036								458	449	438	424						
35	9.12621								460	452	442	429	415					
36	9.45346									455	446	434	420					
37	9.78155									457	449	438	425					
38	10.114									459	451	442	429	416				
39	10.4484									460	454	445	433	421				
40	10.7865										456	447	437	425	413			
41	11.1289										458	450	440	429	416			
42	11.4766										459	452	443	432	420			
43	11.8303										460	454	446	436	424	412		
44	12.1911											455	448	438	427	415		
45	12.56											457	449	441	430	419		
46	12.9381											458	451	443	433	422	411	
47	13.3266											459	452	444	435	424	413	
48	13.7268											460	453	446	437	427	415	
49	14.1401											460	454	447	438	428	418	
50	14.5677											460	455	448	439	430	419	410

The DL6WU graphs also reveal a number of other facts implicit in the data tables. First, the lowest frequency to show a front-to-back peak is 413 MHz in the longest Yagi in the set. As well, none of the peaks actually reaches 460 MHz, due to the fall-off in front-to-back performance above about 455 MHz. The only anomaly in the curves occurs with peak 1, which shows an actual small decrease in frequency before disappearing.

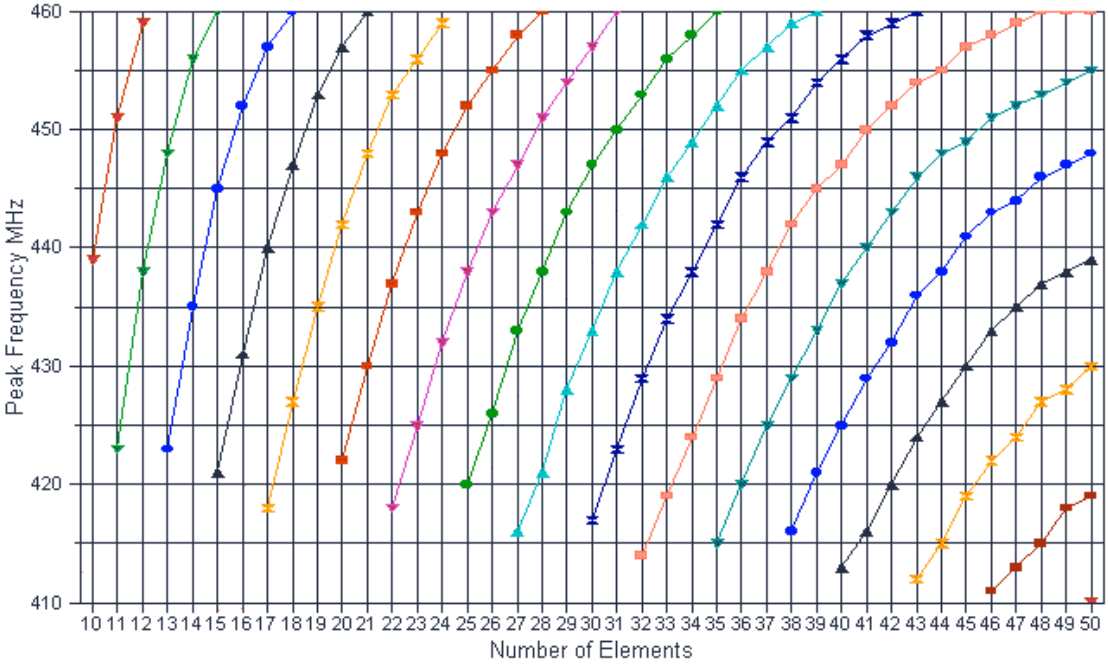

Fig. 24

The curves for the test series of Yagis, shown in **Fig. 24**, are a bit smoother. The peaks are more numerous across the range of boomlengths and numbers of elements, far more numerous than the number of elements or the boomlength range can account for in any simple manner. There are 17 peaks, in contrast to the 10 for the DL6WU series. The ratio of the logs of these numbers only approaches but does not reach the ratio of the number of elements. Of course, there are design differences between the two series, and in this case, the most prominent difference may be in the setting of the spacing between directors.

The test-series graph also shows that 460 MHz is a suitable frequency for a front-to-back peak value. As well, the lowest frequency at which a peak appears is 410 MHz. In the case of both series of Yagis, the frequency region below the lowest peak value is characterized by a leveling of value as a forewarning of a new peak to emerge. These level areas appear when the lowest frequency for a given peak is in the range of about 418 to 423 MHz.

Further information on the front-to-back behavior of the 2 Yagi series is available by inspecting the individual gain/front-to-back graphs that appear in the second part of the overall data accumulation. The data extracted for this preliminary discussion simply includes the information in which I had an immediate interest. Perhaps the most pressing question to me was settling in which direction the front-to-back peaks move as we add new directors.

3. *SWR information*: **Fig. 15** and **Fig. 16** provide samples of the types of graphs that appear in the second section of this data accumulation. The resistance, reactance, and SWR graphs appear together for compactness. However, in this final expedition through the wide-band data, we shall focus solely upon the SWR behavior, using a 50-Ω reference for both antenna series. In general, both Yagi series are capable of very good 70-cm amateur band performance in this category. As well, the resistance and reactance patterns tend to follow the sample. The feedpoint resistance and the feedpoint reactance are just enough out of synchronization with each other to permit a low 50-SWR value across the 420- to 450-MHz range. The SWR climbs slowly below 420 MHz as the resistance and reactance values also change slowly. However, above 450 MHz, both resistance and reactance change both more rapidly and by wider margins. The result is a considerable swing in the SWR values as we approach the upper end of the sweep range.

Wide-Band Performance: WU10-WU40 Yagi Series						Table 13
50-Ohm SWR						
Elements	Bm-Ln	SWR 400	SWR 420	SWR 432	SWR 450	SWR 460
10	2.145068	2.501	1.217	1.317	2.209	2.742
11	2.490042	2.667	1.142	1.092	1.874	4.509
12	2.850003	2.543	1.045	1.273	1.524	5.95
13	3.224951	2.506	1.146	1.39	1.516	6.985
14	3.615028	2.614	1.184	1.342	1.808	7.938
15	4.015049	2.619	1.139	1.195	2.155	8.949
16	4.41507	2.538	1.042	1.046	2.352	9.269
17	4.814946	2.541	1.059	1.15	2.272	10.227
18	5.214967	2.604	1.129	1.258	1.936	10.262
19	5.614988	2.595	1.138	1.269	1.487	9.865
20	6.015008	2.545	1.086	1.181	1.083	9.049
21	6.415029	2.557	1.026	1.044	1.274	7.834
22	6.81505	2.597	1.083	1.093	1.642	6.297
23	7.215071	2.583	1.121	1.198	1.898	4.76
24	7.614947	2.551	1.107	1.229	1.918	4.016
25	8.014968	2.556	1.056	1.172	1.699	4.777
26	8.414989	2.592	1.052	1.067	1.362	6.373
27	8.815009	2.577	1.097	1.074	1.098	7.615
28	9.21503	2.555	1.11	1.166	1.318	8.063
29	9.61505	2.571	1.082	1.204	1.61	7.79
30	10.01507	2.588	1.049	1.166	1.771	6.968
31	10.41495	2.572	1.073	1.083	1.72	5.835
32	10.81497	2.559	1.102	1.073	1.495	4.892
33	11.21499	2.574	1.096	1.148	1.235	4.862
34	11.61501	2.585	1.065	1.186	1.212	5.816
35	12.01503	2.57	1.059	1.16	1.446	6.894
36	12.41505	2.562	1.087	1.093	1.643	7.425
37	12.81507	2.576	1.099	1.077	1.682	7.297
38	13.21495	2.582	1.081	1.137	1.547	6.643
39	13.61497	2.568	1.059	1.173	1.33	5.746
40	14.01499	2.565	1.072	1.155	1.218	5.117

Table 13 provides the basic data on the 50-Ω SWR values across the swept passband from 400 to 460 MHz for the DL6WU Yagi series. The columns listing the SWR values for 420, 432, and 450 MHz establish the relative flatness of the SWR curves within the 70-cm amateur band. However, 2 other columns are especially notable: the 400-MHz SWR values are almost

constant, while the 460-MHz values swing wildly. As we shall see, the upper limit of the SWR passband is actually just above about 455 MHz. Hence, the 460-MHz value lies just outside the range of controlled SWR values, as determined by the Yagi design. Note also that as we shorten the Yagi to its minimum length (10 elements), the value range that is normal for longer versions begins to break down.

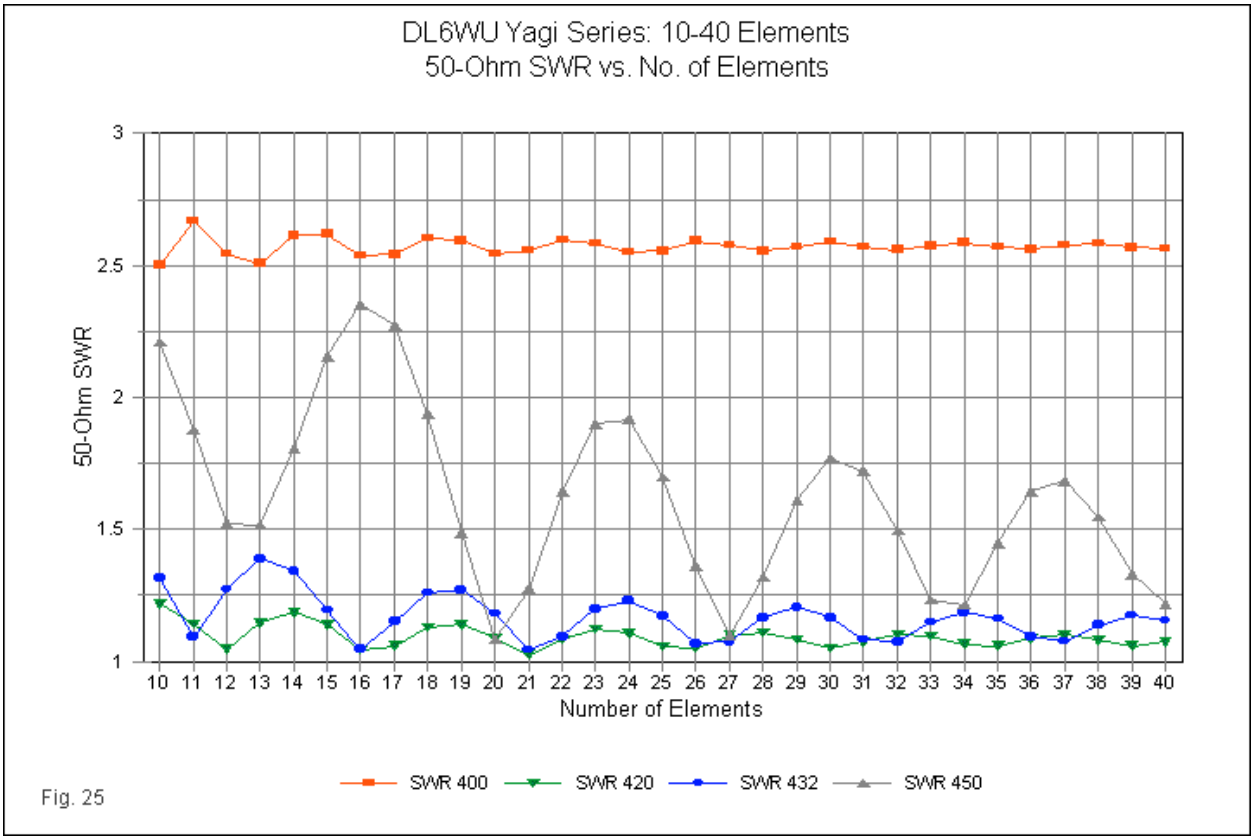

Fig. 25

Fig. 25 graphs the SWR data for all but 460-MHz. I omitted this data because its inclusion would have flattened all other curves and obscured their cyclical nature. The data bears more than a casual resemblance to the front-to-back ratio information in **Fig. 21**. Let's compare a list of the number of cycles at each sampled frequency.

Frequency	Front-Back Ratio	SWR
400 MHz	8 cycles	8 cycles
420 MHz	7 cycles	7.cycles
432 MHz	7 cycles	6 cycles
450 MHz	5 cycles	5 cycles
460 MHz	4 cycles	3 cycles

The tabular data for the test Yagi series appears in **Table 14**. Immediately apparent is the fact the, like the DL6WU series, the test series values for 420 through 450 MHz are flat, and the values for 400 MHz are both nearly constant and only about 0.1 greater than for the DL6WU series. However, the 460-MHz value swings only over a much more modest range of values. In fact, the SWR passband for the test series of Yagis is slightly greater than for the DL6WU series, with its upper limits above 460 MHz. How we know this fact will become apparent shortly.

Wide-Band Performance: LB10 to LB50 Yagi Series						Table 14
50-Ohm SWR						
Elements	Bm-Ln	SWR 400	SWR 420	SWR 432	SWR 450	SWR 460
10	1.52962	2.608	1.294	1.249	1.975	3.558
11	1.77685	2.632	1.124	1.418	1.486	1.456
12	2.02258	2.664	1.245	1.177	1.682	2.466
13	2.28	2.61	1.072	1.34	1.593	2.9
14	2.54783	2.655	1.217	1.172	1.306	1.257
15	2.82488	2.633	1.038	1.233	1.603	2.226
16	3.11004	2.622	1.179	1.236	1.356	2.689
17	3.40226	2.668	1.101	1.095	1.277	1.48
18	3.70057	2.59	1.104	1.246	1.513	1.786
19	4.00408	2.688	1.156	1.123	1.284	2.612
20	4.31197	2.588	1.007	1.135	1.216	1.937
21	4.6235	2.669	1.144	1.215	1.455	1.305
22	4.93798	2.624	1.101	1.061	1.3	2.273
23	5.25483	2.625	1.062	1.153	1.134	2.397
24	5.57352	2.663	1.144	1.187	1.398	1.502
25	5.89361	2.601	1.055	1.029	1.349	1.635
26	6.21472	2.663	1.098	1.159	1.088	2.437
27	6.53657	2.623	1.127	1.166	1.322	2.129
28	6.85891	2.629	1.031	1.014	1.391	1.304
29	7.1816	2.656	1.118	1.161	1.144	1.934
30	7.50457	2.609	1.104	1.151	1.228	2.464
31	7.82782	2.657	1.045	1.017	1.404	1.848
32	8.15142	2.626	1.126	1.163	1.236	1.339
33	8.47553	2.629	1.078	1.139	1.128	2.192
34	8.80036	2.654	1.069	1.025	1.378	2.387
35	9.12621	2.613	1.125	1.163	1.326	1.595
36	9.45346	2.651	1.058	1.132	1.076	1.512
37	9.78155	2.632	1.087	1.026	1.297	2.337
38	10.114	2.624	1.12	1.159	1.395	2.303
39	10.4484	2.654	1.05	1.139	1.196	1.509
40	10.7865	2.62	1.092	1.004	1.14	1.528
41	11.1289	2.636	1.118	1.14	1.37	2.303
42	11.4766	2.649	1.055	1.161	1.375	2.431
43	11.8303	2.618	1.079	1.057	1.175	1.839
44	12.1911	2.637	1.12	1.075	1.132	1.258
45	12.56	2.649	1.086	1.163	1.341	1.663
46	12.9381	2.623	1.044	1.158	1.445	2.317
47	13.3266	2.625	1.091	1.08	1.409	2.719
48	13.7268	2.648	1.122	1.02	1.302	2.801
49	14.1401	2.647	1.112	1.108	1.221	2.701
50	14.5677	2.627	1.075	1.177	1.259	2.589

The graphing of the data in the table, in **Fig. 26**, reveals that the test series also has a cyclical structure, just as did the test series front-to-back ratio data. As well, the cycles are still evident even if we include the data for 460 MHz, although the lines for the lower frequencies of the sampling require careful scrutiny to keep them sorted. As well, we find the same DL6WU characteristic of the normal curves beginning to break down as we shorten the Yagi toward its minimum length of 10 elements. Only at 10 elements does the 50-Ω SWR approach 2:1. However, the SWR within the 70-cm amateur band for all Yagi lengths is extremely flat and well behaved.

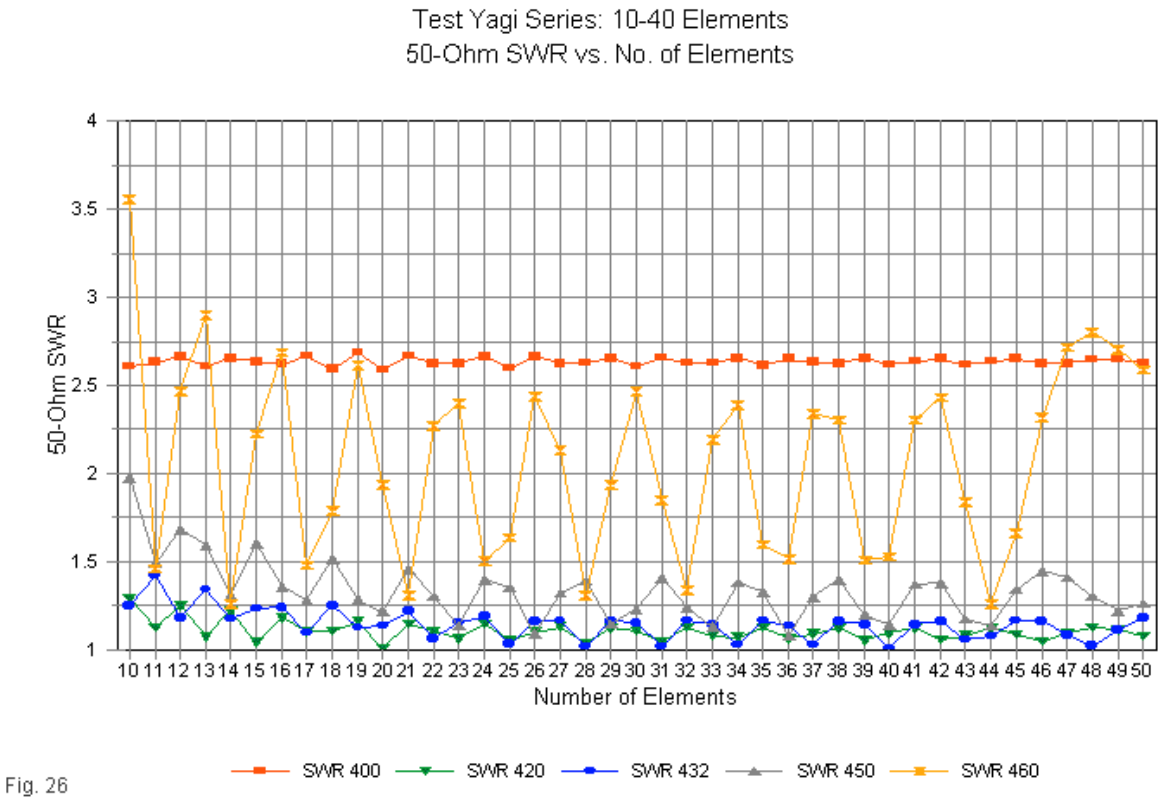

Fig. 26

As we did for the DL6WU series, let's compare the number of cycles at each sampled frequency for the test series. Once more, there appears to more than a casual resemblance between the periodic fluctuations in the front-to-back and the SWR data sets.

Frequency	Front-Back Ratio	SWR
400 MHz	15 cycles	15 cycles
420 MHz	15 cycles	15.cycles
432 MHz	14 cycles	14 cycles
450 MHz	12 cycles	12 cycles
460 MHz	12 cycles	11 cycles

When gathering more detailed information on the wide-band behavior of the front-to-back ratio, counting peak 180° values proved to be very convenient. Wide-band SWR curves require a reverse treatment: counting "dips" in the SWR value, where a dip is a lower 50-Ω SWR value at a given frequency than at either adjacent frequency. Like the front-to-back ratio peaks, the SWR dips tend to increase in number as we increase the boomlength and number of elements. This phenomenon indicates that there is a compression of the frequency span between dips as we increase the Yagi length. As well, the curves appear as a series of individual dips that emerge at a lower frequency for a shorter Yagi and eventually disappear at the higher frequency for a longer array.

Table 15 shows the dip frequency data for the DL6WU series of Yagis. Like the front-to-back table of peak frequencies (**Table 11**), the SWR table displays 10 distinct lines of note for this beam series. Also like the front-to-back series, the lines are relatively but not perfectly smooth.

Wide-Band Performance: WU10-WU40 Yagi Series											Table 15
50-Ohm SWR Dips and Frequencies											
Elements	Bm-Ln	Dip 1	Dip 2	Dip 3	Dip 4	Dip 5	Dip 6	Dip 7	Dip 8	Dip 9	Dip 10
10	2.145068	455	444	426							
11	2.490042	456	447	432	417						
12	2.850003	457	449	436	420						
13	3.224951	458	450	440	423						
14	3.615028	458	451	442	426	417					
15	4.015049	458	452	443	429	417					
16	4.41507	459	453	444	432	419					
17	4.814946	459	453	446	435	421					
18	5.214967	459	454	447	437	424					
19	5.614988	459	454	448	440	426	417				
20	6.015008	459	455	450	442	429	418				
21	6.415029	459	455	451	443	431	420				
22	6.81505	459	456	452	444	434	422				
23	7.215071	459		452	445	436	424				
24	7.614947	459		453	446	438	427	418			
25	8.014968	459		453	447	440	429	420			
26	8.414989	459		454	449	442	431	421			
27	8.815009	459		454	450	443	433	423			
28	9.21503	459		455	451	444	435	425			
29	9.61505	459			452	445	437	427	419		
30	10.01507	459			453	446	439	429	420		
31	10.41495	459			453	447	441	431	422		
32	10.81497	459			453	448	442	433	423		
33	11.21499	459			454	449	444	434	425	419	
34	11.61501	459			454	451	445	436	427	420	
35	12.01503	459			454	452	445	438	429	421	
36	12.41505	459				452	446	440	431	422	
37	12.81507	459				453	447	442	432	424	
38	13.21495	459				453	448	443	434	426	419
39	13.61497	459				453	449	444	436	428	420
40	14.01499	459				454	450	444	438	429	422

One data column requires special comment. The highest-frequency SWR dip remains constant throughout the series of frequency sweeps. At the shortest beam lengths, it shows a rising frequency as we lengthen the Yagi. By 16 elements, it arrives and stays at 459 MHz. All other SWR dips emerge and disappear when passing about 456 MHz. This phenomenon is no illusion. For Yagi sizes just past the disappearance of a dip, the SWR value between the next dip and 459 MHz shows a flattening or stair-stepping to indicate where a dip might be if there were one or if we had used an increment of frequency sweep under 1 MHz. Perhaps the most likely explanation for the oddity, which shows up clearly in **Fig. 27**, is that the SWR dip at 459 MHz lies outside the range of impedance values controlled by the DL6WU design. The constant 459-MHz dip also shows that the DL6WU SWR passband has an upper limit lower than this frequency. Beyond the upper-most dip, the SWR values swing wildly, but only decrease below 3:1 for the 10-element version of the Yagi.

Another notable feature revealed by the graphed values is the fact that above 440 MHz, the lines bend to a slightly more horizontal angle. The line shape indicates that above about 440 MHz, the rate of change of the dip frequency slows as we add new directors. In fact, there is a slight S-shape to some of the curves, indicating that at the lowest frequencies, the initial rate of dip frequency increase is also slow. Since the lowest frequency of dip appearance is about 417 MHz, we can only glimpse this rate. Between about 420 and 440 MHz, the rate of dip frequency increase is nearly linear with the addition of new directors. Similar trends show in the DL6WU front-to-back graph (**Fig. 23**), although the S-shaping of the curves is far less vivid. The data does not make self-evident what these characteristics may imply about trimming Yagi design in general or about the DL6WU series in particular.

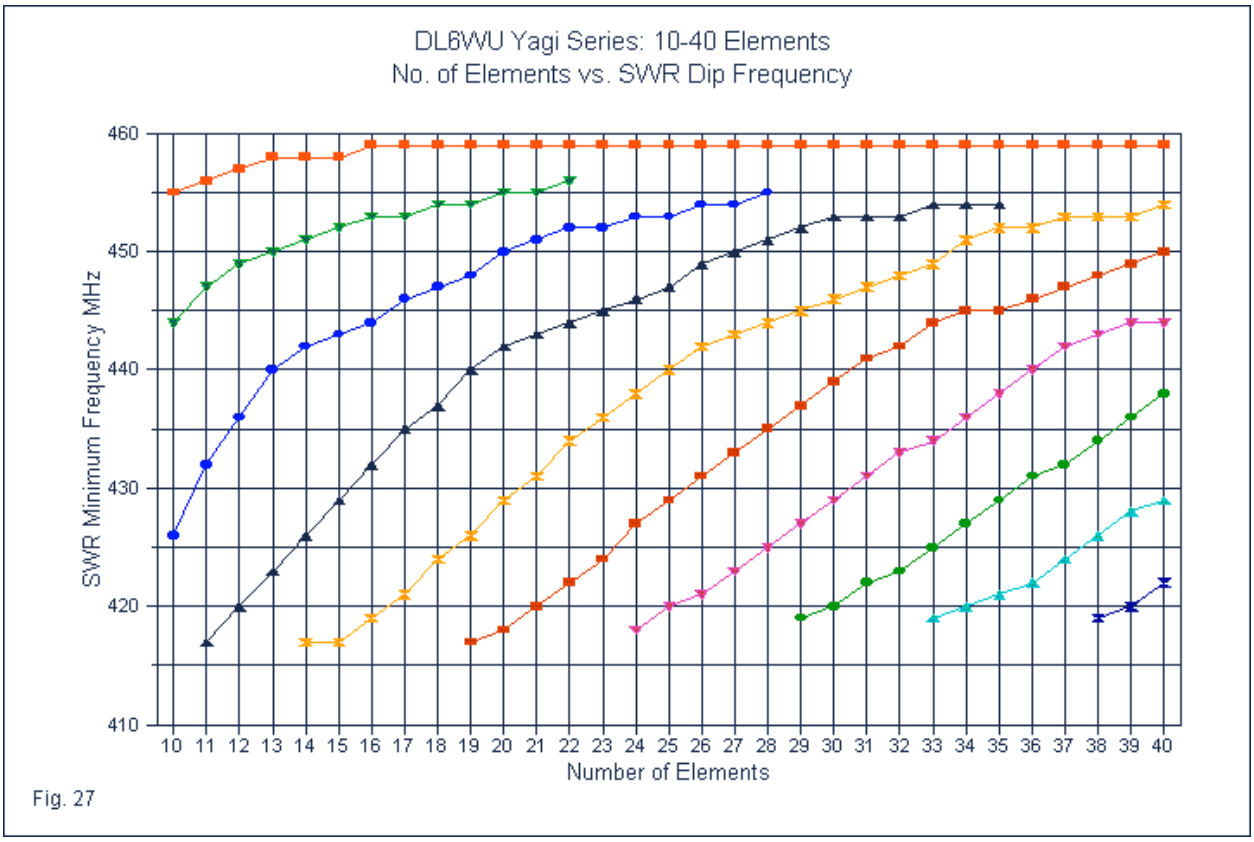

Fig. 27

Table 16 presents the corresponding "dip" data for the test series of Yagis. The table appears twice: in shrunken portrait form for screen readers and again in landscape form for paper readers.

Wide-Band Performance: LB10 to LB50 Yagi Series — Table 16

50-Ohm SWR Dips and Frequencies

Elements	Bm-Ln	Dip 1	Dip 2	Dip 3	Dip 4	Dip 5	Dip 6	Dip 7	Dip 8	Dip 9	Dip 10	Dip 11	Dip 12	Dip 13	Dip 14	Dip 15	Dip 16	Dip 17	Dip 18
10	1.52962	457	441	431	414														
11	1.77685	459	449	438	421														
12	2.02258		454	442	430	415													
13	2.28		457	447	437	421													
14	2.54783		460	451	441	428	415												
15	2.82488			455	444	435	419												
16	3.11004			457	448	440	426												
17	3.40226			459	452	442	433	418											
18	3.70057				455	445	437	423											
19	4.00408				457	448	441	429	417										
20	4.31197				459	452	443	434	420										
21	4.6235				460	454	445	438	425										
22	4.93798					456	448	441	431	418									
23	5.25483					458	451	443	435	422									
24	5.57352					459	453	445	438	426									
25	5.89361					460	455	447	441	431	419								
26	6.21472						457	450	443	436	423								
27	6.53657						458	452	445	438	427	417							
28	6.85891						460	455	447	441	432	420							
29	7.1816							456	449	443	436	423							
30	7.50457							458	452	444	438	428	418						
31	7.82782							459	454	446	441	432	421						
32	8.15142							460	455	448	443	436	424						
33	8.47553								457	451	444	438	429	419					
34	8.80036								458	453	446	440	432	422					
35	9.12621								459	455	448	442	436	425	418				
36	9.45346								460	456	450	444	438	429	419				
37	9.78155									457	452	445	440	433	422				
38	10.114									458	454	447	442	435	425	418			
39	10.4484									459	455	449	443	438	429	420			
40	10.7865									460	457	451	445	440	432	422			
41	11.1289										457	452	446	441	435	425	418		
42	11.4766										458	454	448	443	437	428	420		
43	11.8303										459	455	449	444	439	431	422		
44	12.1911										460	456	451	445	440	433	424	418	
45	12.56											457	452	446	441	435	426	419	
46	12.9381											457	453	447	442	437	429	420	
47	13.3266											458	454	448	443	438	431	422	
48	13.7268											458	454	449	444	439	432	423	417
49	14.1401											459	455	450	444	440	433	425	418
50	14.5677											459	455	450	444	440	434	426	419

Wide-Band Performance: LB10 to LB50 Yagi Series																			Table 16
50-Ohm SWR Dips and Frequencies																			
Elements	Bm-Ln	Dip 1	Dip 2	Dip 3	Dip 4	Dip 5	Dip 6	Dip 7	Dip 8	Dip 9	Dip 10	Dip 11	Dip 12	Dip 13	Dip 14	Dip 15	Dip 16	Dip 17	Dip 18
10	1.52962	457	441	431	414														
11	1.77685	459	449	438	421														
12	2.02258		454	442	430	415													
13	2.28		457	447	437	421													
14	2.54783		460	451	441	428	415												
15	2.82488			455	444	435	419												
16	3.11004			457	448	440	426												
17	3.40226			459	452	442	433	418											
18	3.70057				455	445	437	423											
19	4.00408				457	448	441	429	417										
20	4.31197				459	452	443	434	420										
21	4.6235				460	454	445	438	425										
22	4.93798					456	448	441	431	418									
23	5.25483					458	451	443	435	422									
24	5.57352					459	453	445	438	426									
25	5.89361					460	455	447	441	431	419								
26	6.21472						457	450	443	436	423								
27	6.53657						458	452	445	438	427	417							
28	6.85891						460	455	447	441	432	420							
29	7.1816							456	449	443	436	423							
30	7.50457							458	452	444	438	428	418						
31	7.82782							459	454	446	441	432	421						
32	8.15142							460	455	448	443	436	424						
33	8.47553								457	451	444	438	429	419					
34	8.80036								458	453	446	440	432	422					
35	9.12621								459	455	448	442	436	425	418				
36	9.45346								460	456	450	444	438	429	419				
37	9.78155									457	452	445	440	433	422				
38	10.114									458	454	447	442	435	425	418			
39	10.4484									459	455	449	443	438	429	420			
40	10.7865									460	457	451	445	440	432	422			
41	11.1289										457	452	446	441	435	425	418		
42	11.4766										458	454	448	443	437	428	420		
43	11.8303										459	455	449	444	439	431	422		
44	12.1911										460	456	451	445	440	433	424	418	
45	12.56											457	452	446	441	435	426	419	
46	12.9381											457	453	447	442	437	429	420	
47	13.3266											458	454	448	443	438	431	422	
48	13.7268											458	454	449	444	439	432	423	417
49	14.1401											459	455	450	444	440	433	425	418
50	14.5677											459	455	450	444	440	434	426	419

Like the DL6WU data on SWR dips, the test series table shows many similarities to the front-to-back table (**Table 12**). Two items deserve special note. First, the SWR table shows 18 detectable dip lines, compared to 17 lines for the front-to-back ratio table. Both of these numbers contrast to the 10 distinct lines that appear on both DL6WU tables. Second, if we draw a pair of lines connecting all of the highest frequency values and all of the lowest frequency values, the lines will have very similar shapes in both tables. The lines will not be linear.

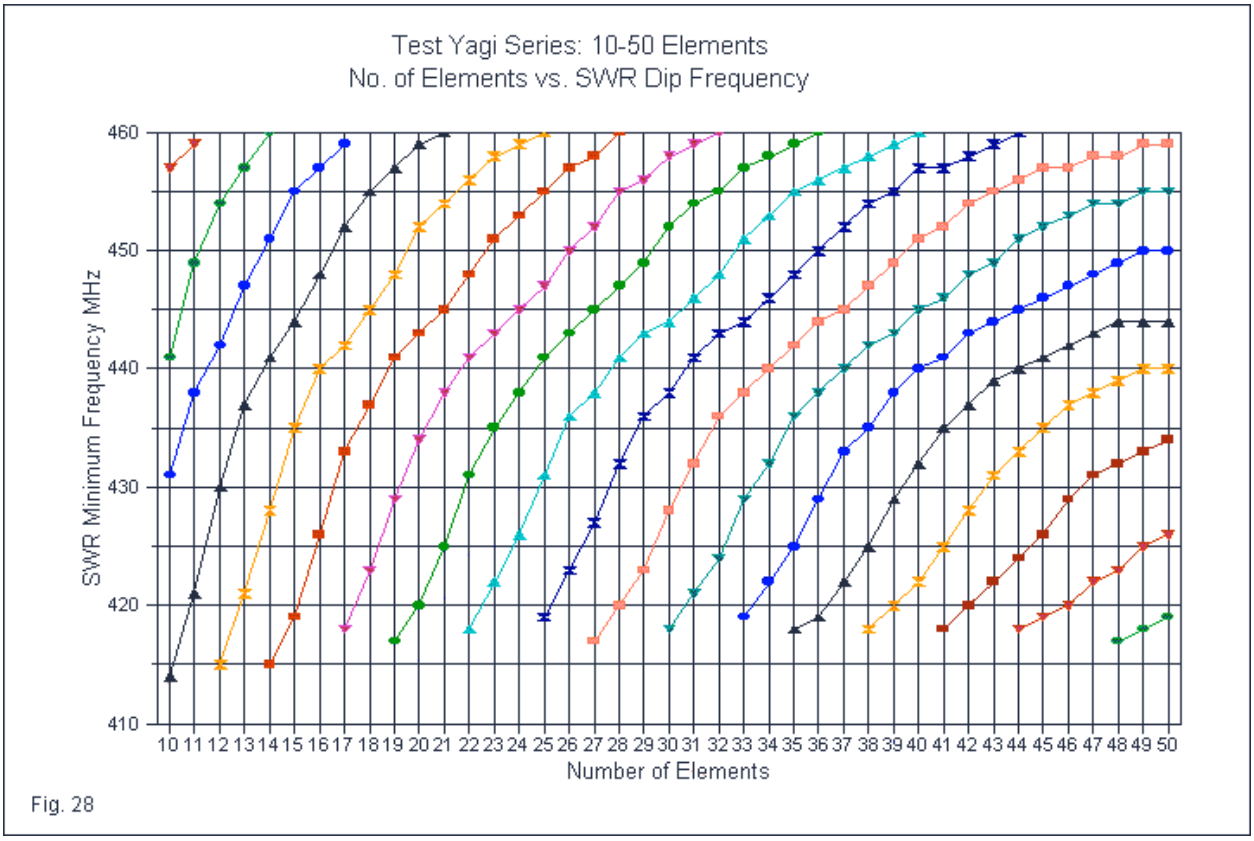

Fig. 28 graphs the SWR dip frequency lines from the tabular data. Note that 460 MHz is a valid frequency for all lines, indicating that the disappearance of the dip lies on or above this frequency. If there is an SWR passband limit to the SWR dip for the test series, it lies above the limit chosen for the frequency sweeps. Hence, the test series of Yagis has an SWR passband slightly greater than the DL6WU series. However, within the 70-cm amateur band, both series exhibit very well controlled SWR values.

Like the DL6WU SWR lines, the test series lines show a fairly distinct S shape, indicating a slower rate of dip frequency change at both the lower and higher ends of the sweep range. It is difficult to detect a distinct knee in the upper end of the curves, but it appears to be at about 435 MHz, slightly lower than for the DL6WU curves. The curves at all frequencies tend to flatten at the longest boomlengths, perhaps in relationship to the widening space between the forward-most directors.

The most vivid contrast between the DL6WU and test series lies in the number of dips at any given frequency within the sweep. From 10 to 40 elements, the DL6WU series shows a range of 3 to 7 dips (including the limiting dip). The test series shows 4 to 8 dips over its element

range of 10 to 50 elements. As noted throughout, the shortest test series Yagi is more than 0.5 λ shorter than the shortest DL6WU beam, while the longest test series array is almost 0.5 λ longer than the 40-element DL6WU version.

Undoubtedly, there are many other characteristics of the SWR data--and, indeed, of all of the data--that deserve attention. These notes, tables, and graphs only call attention to a small part of the information contained in the series of frequency sweeps over each member of each trimming Yagi series. The basic sweep graphs in the second part of these data accumulation notes may provide other clues to better understanding trimming Yagi behavior. If they prove insufficient, then the tables of Yagi dimensions allow for independent modeling of the beams for the derivation of other data. Among the data that we have not examined very closely is the feedpoint resistance and reactance. We saw, for example, some level of correlation between the SWR and front-to-back behavior of both series of beams. A close examination of the resistance and reactance data might well turn up other and possibly tighter correlations.

Having exhausted available energy for the wide-band study of the arrays, we should briefly examine one final question.

The Element Diameter Question

Early on, we noted that the program dl6wu-gg.exe accepts a wide range of element diameters as a function of a wavelength. For this exercise we selected 4 mm at 432 MHz or 0.005764 λ. Since we had two comparative Yagi series to examine, a common element diameter seemed prudent. We also noted that the dl6wu-gg.exe program accepts diameters in a step-wise arrangement. The system is practical, if imprecise compared to separately calculating the required element lengths for a new diameter based upon the element reactance.

Of course, the DL6WU series of Yagis uses the same spacing between elements regardless of element diameter. Over the 20:1 range of element diameters accepted by the program, the adjustment of element length alone will not capture all of the inter-element coupling, and hence departures from the mid-range curves in this exercise are bound to result. The question is whether smaller excursions in element diameter will also show such departures.

To test this potential, I created two new 432-MHz DL6WU Yagis from the program. One used 2-mm diameter elements, and the other used 8-mm diameter elements. The element lengths come directly from the program. All of the Yagis use 20 elements total. As a check upon those dimensions, I used the basic 4-mm Yagi and converted the element lengths for an 8-mm diameter via the normal reactance equations as described in RSGB's *The VHF/UHF DX Book*, page 7-28. First, we obtain the original element's reactance, X, in Ohms.

$$X_\Omega = \left[430.3 \log_{10}\left(\frac{2\lambda}{D}\right) - 320\right]\left(\frac{2L}{\lambda} - 1\right) + 40$$

D is the (original) diameter, L is the length, and λ is a wavelength, all in the same unit of measure. To find the new length, we reverse the process, using the value of reactance.

$$L = \left[\frac{X - 40}{430.3 \log_{10}\left(\frac{2\lambda}{D}\right) - 320} + 1\right]\frac{\lambda}{2}$$

L and D, of course, refer to the new length and diameter and are in the same unit of measure as λ. The Basic collection of utility programs maintained by George Murphy, VE3ERP--HAMCALC-

-contains a convenient program for batch-calculating the 20 conversions. The results of the conversion yielded a 20-element Yagi with slightly different element lengths from those produced by dl6wu-gg.exe. So the net yield was a total of 4 20-element DL6WU Yagis, WU20-2, WU-20-4, and WU20-8 from the program, and WU20-8A from the conversion of 4-mm elements to 8-mm elements. **Table 17** provides the dimensions both in millimeters and in wavelengths for all 4 models.

DL6WU 20-Element Yagi in 3 Diameters				From dl6wu-gg.exe						From Scaling Equations		
				WL	mm	WL	mm	WL	mm	WL	mm	
				Diameter	Diameter	Diameter	Diameter	Diameter	Diameter	Diameter	Diameter	
		WL	mm	0.002882	2 mm	0.005764	4 mm	0.011528	8 mm	0.011528	8 mm	
Element	El. Name	Boom Len	Boom Len	El. Len	El. Len	El. Len	El. Len	El. Len	El. Len	El. Len	El Len	
1	Reflector	0	0	0.487475	338.29	0.487057	337.9999	0.484463	336.2	0.484449	336.19	
2	Driver	0.20001	138.8	0.483354	335.43	0.479333	332.64	0.473785	328.79	0.475169	329.75	
3	D1	0.274942	190.8	0.447559	310.59	0.436132	302.66	0.422846	293.44	0.423278	293.74	
4	D2	0.455067	315.7999	0.443625	307.86	0.43106	299.14	0.417558	289.77	0.417183	289.51	
5	D3	0.670063	464.9999	0.439245	304.82	0.425901	295.56	0.411347	285.46	0.410987	285.21	
6	D4	0.919932	638.4	0.434979	301.86	0.421002	292.16	0.405583	281.46	0.405107	281.13	
7	D5	1.200062	832.7998	0.431146	299.2	0.41665	289.14	0.400583	277.99	0.399877	277.5	
8	D6	1.499933	1040.9	0.427803	296.88	0.412874	286.52	0.396274	275	0.395338	274.35	
9	D7	1.814935	1259.5	0.424864	294.84	0.409618	284.26	0.399761	277.42	0.391432	271.64	
10	D8	2.145068	1488.6	0.422327	293.08	0.406736	282.26	0.389314	270.17	0.38796	269.23	
11	D9	2.490042	1728	0.420065	291.51	0.404171	280.48	0.386432	268.17	0.384876	267.09	
12	D10	2.850003	1977.799	0.417904	290.01	0.401894	278.9	0.383867	266.39	0.382152	265.2	
13	D11	3.224951	2238	0.416189	288.82	0.399819	277.46	0.381533	264.77	0.379659	263.47	
14	D12	3.615028	2508.699	0.414517	287.66	0.397917	276.1399	0.3794	263.29	0.377368	261.88	
15	D13	4.015049	2786.299	0.412961	286.58	0.396188	274.9399	0.377455	261.94	0.375293	260.44	
16	D14	4.41507	3063.9	0.411534	285.59	0.394574	273.82	0.375639	260.68	0.360379	250.09	
17	D15	4.814946	3341.399	0.410194	284.66	0.393046	272.7599	0.373953	259.51	0.371518	257.82	
18	D16	5.214967	3618.999	0.408955	283.8	0.391663	271.7999	0.372368	258.41	0.369861	256.67	
19	D17	5.614988	3896.6	0.407788	282.99	0.390337	270.88	0.370884	257.38	0.368261	255.56	
20	D18	6.015008	4174.199	0.406678	282.22	0.389069	270	0.369486	256.41	0.366748	254.51	Table 17

The question is what, if any, performance differences exist among the models. Like all other NEC-4 models in the study, we may compare them using a free-space environment. The comparison will tell us whether the curves that we have accumulated by consolidating data are general or whether they are specific to the original 4-mm element models.

In advance, we might bring to the exercise some suspicions. For most antenna designs, we expect otherwise identical antennas to show a wider operating bandwidth in most performance categories for larger-diameter elements and, conversely, a narrower operating bandwidth for smaller-diameter elements. Therefore, we expect the gain curve for the 2-mm version of the antenna to have lower gain at the passband limits than the 4-mm version.

However, some operating parameters are not controlled closely by the design and exhibit cycles of minimum-to-maximum value shifts. The 180° front-to-back ratio and the feedpoint parameters (resistance, reactance, and 50-Ω SWR) are cases in point. The peak values might occur at the same frequencies for all of the antenna versions, with variation showing up only in the strength of peak values. Alternatively, the cycles might contract or expand--for smaller or larger diameter elements. The latter alternative would alter for many DL6WU boomlengths where the design frequency falls on a particular cycle's curve. A third alternative is that the new diameters produce altogether different performance curves.

Table 18 presents for the 4 models the same information as previously used in the study: the single-unit performance at the design frequency and wide-band data for gain, front-to-back ratio, and 50-Ω SWR. From that data, we can gather a sense of what may actually occur by overlaying the frequency sweep graphs in various categories of operation. Of importance is the reminder that all models represent a 20-element 432-MHz DL6WU Yagi.

DL6WU 20-Element Yagi in 3 Diameters													Table 18
Single-Unit Free-Space Performance at 432 MHz													
Model	Bm-Ln	Gain	180 F-B	H BW	H F/SL	V BW	V F/SL	FP Resis	FP React	SWR-50			
WU20-2	6.015008	17.52	25.39	25.2	17.06	26.4	15.16	51.24	11.08	1.246			
WU20-4	6.015008	17.43	24.37	25.8	17.16	26.8	15.17	50.63	8.346	1.181			
WU20-8	6.015008	17.55	31.08	25.6	17.84	26.6	15.97	55.95	10.82	1.262			
WU20-8A	6.015008	17.39	24.79	26.4	18.35	27.4	16.39	50.99	9.954	1.219			
Wide-Band Gain Performance													
Model	400	420	432	Pk Gain	PG-G432	Pk Gn Fq	450	Delta Gn	460				
WU20-2	11.66	16.29	17.59	17.66	0.07	435	15.88	1.78	-0.62				
WU20-4	13.13	16.32	17.43	17.69	0.26	437	16.77	1.37	10.83				
WU20-8	14.34	16.62	17.55	17.68	0.13	436	16.94	1.06	15.43				
WU20-8A	14.16	16.41	17.39	17.65	0.26	438	17.3	1.24	16.24				
Wide-Band Front-to-Back Ratio Performance													
Model	400	420	432	450	460	No. Pks	180-Degree Peak Frequencies - |						
WU20-2	6.84	17.38	25.39	19.39	11.56	6	460	457	454	447	434	417	
WU20-4	9.38	18.98	24.37	27.88	10.06	4		458		450	434	416	
WU20-8	12.25	20.17	31.08	22.53	18.76	4		459		452	433	414	
WU20-8A	12.51	18.92	24.79	20.49	16.98	3				452	434	414	
Wide-Band 50-Ohm SWR Performance													
Model	400	420	432	450	460	No. Dips	SWR Dip Frequencies - |						
WU20-2	3.621	1.105	1.246	1.629	97.598	7	457	454	451	447	440	429	420
WU20-4	2.545	1.086	1.181	1.083	9.049	6	459	455			442	429	418
WU20-8	1.837	1.066	1.262	1.117	3.656	5		455		450	442	427	418
WU20-8A	1.778	1.113	1.219	1.412	2.102	5		458	452			428	416

At the design frequency, we may note that the gain value for the re-calculated version, 8A, is closer to the original 4-mm model than is the gain value for the 8-mm program design. So too are the 180° front-to-back ratio and the feedpoint resistance and reactance values. Indeed, model 8A shows a wider beamwidth in both planes than the original 4-mm model, while the program design shows a narrower beamwidth. Even with a narrower beamwidth, the program's 8-mm design reports a better front-to-sidelobe ratio than the 4-mm antenna. However, the re-calculated version (8A) gives us the best front-to-sidelobe ratios of the lot.

The parallelism of design frequency performance values between the original model and its re-calculated 8-mm cousin comes at a price that only appears when we examine the frequency sweep data. **Fig. 29** overlays the gain data for all 4 models.

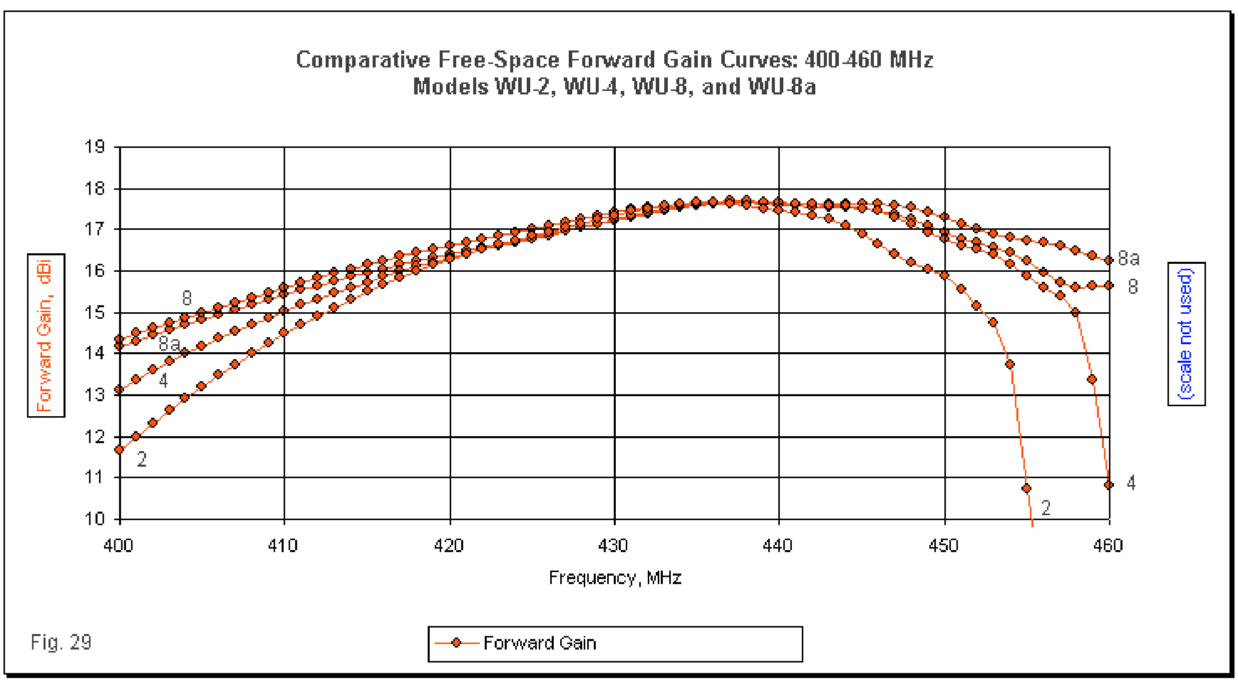

Fig. 29

The curves for the 2-mm and 4-mm versions of the antenna show the narrower bandwidth that we initially suspected. In fact, the 2-mm gain at 460 MHz is under 0 dB. All of the models show a generally similar frequency of peak gain. However, the re-calculated 8-mm version (model 8A) shows a bias upward in the pass band. Hence, its gain at 400 MHz is lower than the gain of model 8, and its peak gain region plateaus to nearly 446 MHz. As a result, its value for ΔGain (the difference between the maximum and minimum gain values within the 70-cm amateur band) is higher than for model 8, the program-derived 8-mm antenna.

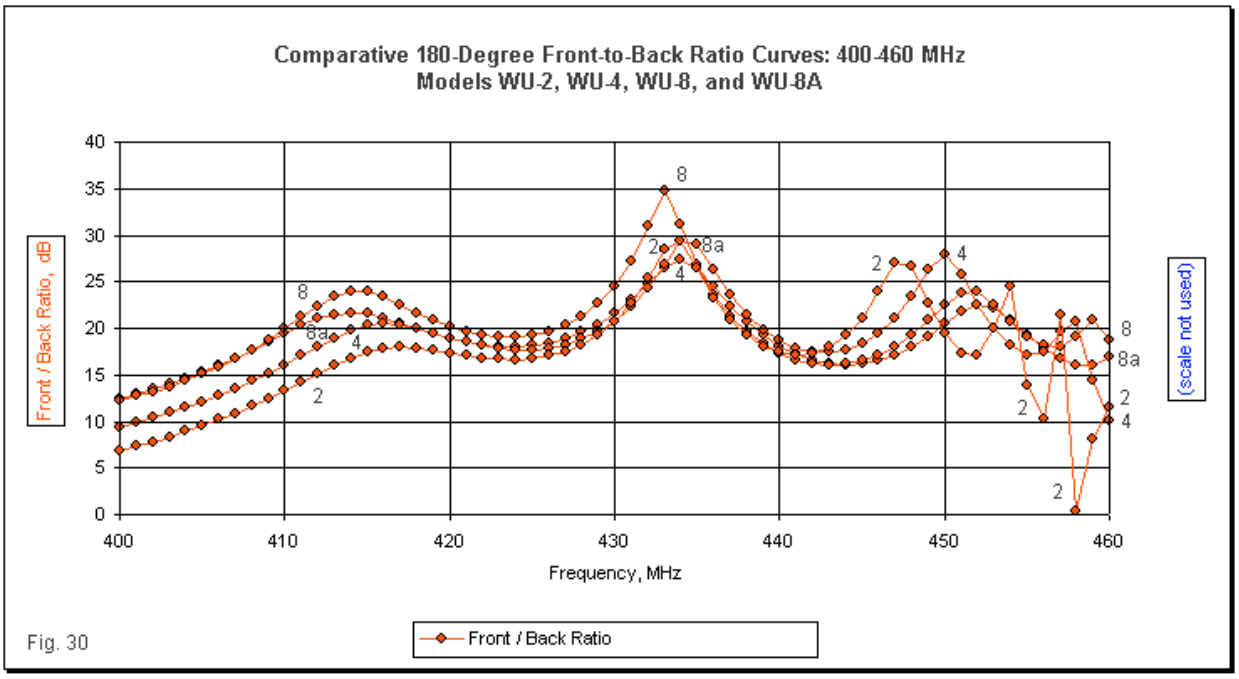

Fig. 30

In **Fig. 30**, we find an overlay of the 4 frequency sweep front-to-back curves. The region in the vicinity of the design frequency shows only small offsets in frequency from one curve to the next. However, since the front-to-back peak occurs near the design frequency for this boomlength, small offsets in peak frequency can yield larger differences in the design frequency value.

Most of the curve compression or spreading that accompanies smaller or larger diameter elements occurs below 420 MHz and above 440 MHz. At the lower end of the sweep passband, the displacement of the peak front-to-back value among the models is more apparent. However, the greatest changes occur high in the passband. The extra peaks of the 2-mm version are readily apparent, although the ones with the highest frequencies may fall outside the usable gain passband for that version of the Yagi. Equally apparent is the effect of the seemingly slight bias of the re-calculated 8-mm version of the antenna. It shows only 3 front-to-back peaks within the sweep passband, in contrast to 4 peaks for the program-derived version with the same element diameter.

In the tabular data, we note that not all peaks have counterparts from one antenna version to the next. Hence, the placement of the seeming counterpart front-to-back peaks is only a "best guess." It likely would require a large series of models using element diameters that increase from 2 to 8 mm in small increments in order to establish the exact characteristics of the peaks. In the SWR data at the bottom of **Table 18**, we find a similar situation of guessing at which dips correspond among the models.

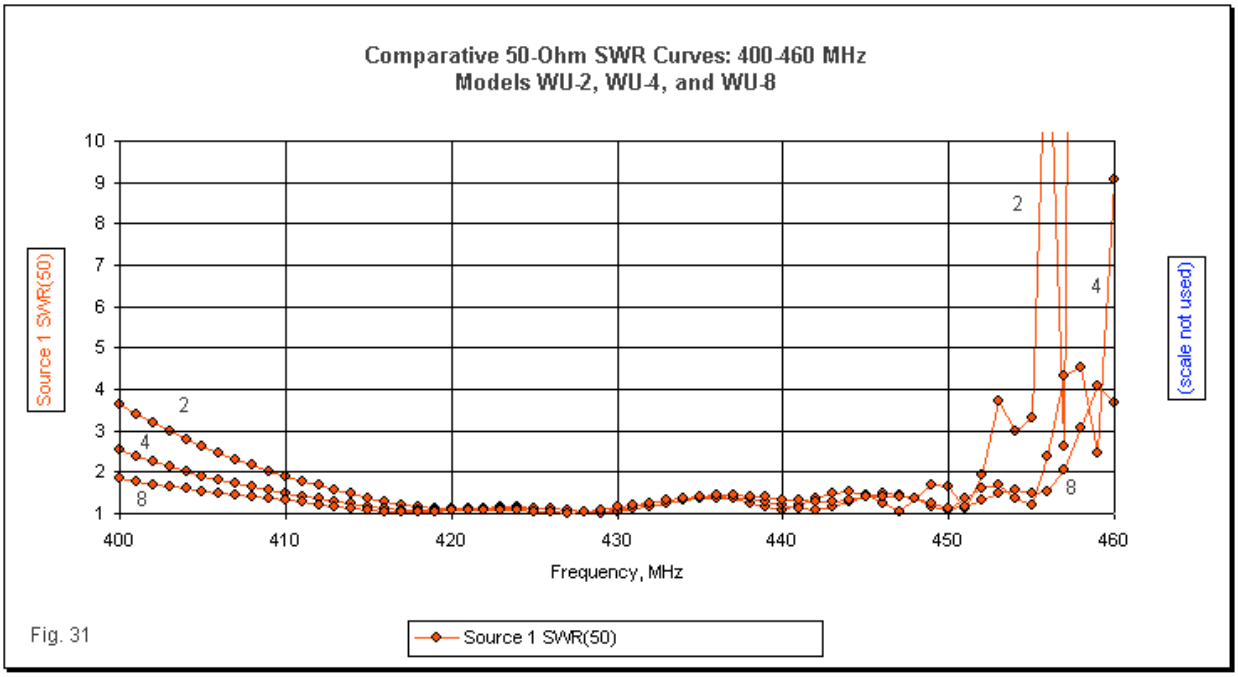

Fig. 31 provides 50-Ω SWR overlays for the 3 models derived from the dl6wu-gg.exe program. The lower end of the spectrum shows an easily anticipated rise in SWR as we reduce the element diameter. Since operating characteristics change slowly below the design frequency, the curves appear to be quite orderly. We cannot report the same conclusion about the SWR behavior above 440 MHz. At the upper end of the spectrum, we find an extreme compression of narrow SWR cycles as we reduce the element diameter. However, note the last small peak in each SWR sequence. The curves have similar shapes for all 3 versions of the antenna, but the last small peak occurs at a lower frequency with reduced element diameters.

Adding the 4th SWR curve for the recalculated version of the 8-mm Yagi (model 8A) to **Fig. 31** would only have served to obscure the data for the other three versions. **Fig. 32** uses an expanded scale and contains only the SWR curves for models 8 and 8A, the 2 8-mm element diameter Yagis. We may first note two general properties of the 8A version. First, its overall SWR level throughout the sweep passband is lower than for the program-derived model 8. Second, up to about 440 MHz or so, its curves generally track with the other models in the overall sequence.

Above 440 MHz, the bias of the re-calculated 8-mm Yagi toward higher frequency performance becomes apparent in the SWR curves. Model 8A has only 4 SWR dip points, and the ones at the upper end of the spectrum occur at higher frequencies than the corresponding dips for the program-derived model. In fact, model 8 from the program manages to squeeze in 3 dips in the spectrum occupied by 2 dips for model 8A. As a result, the value of SWR at 460 MHz is much higher for model 8, high enough to mark a position outside the operating passband. In contrast, model 8A remains operable at less than 2:1 50-Ω SWR all the way from below 400 MHz to above 460 MHz.

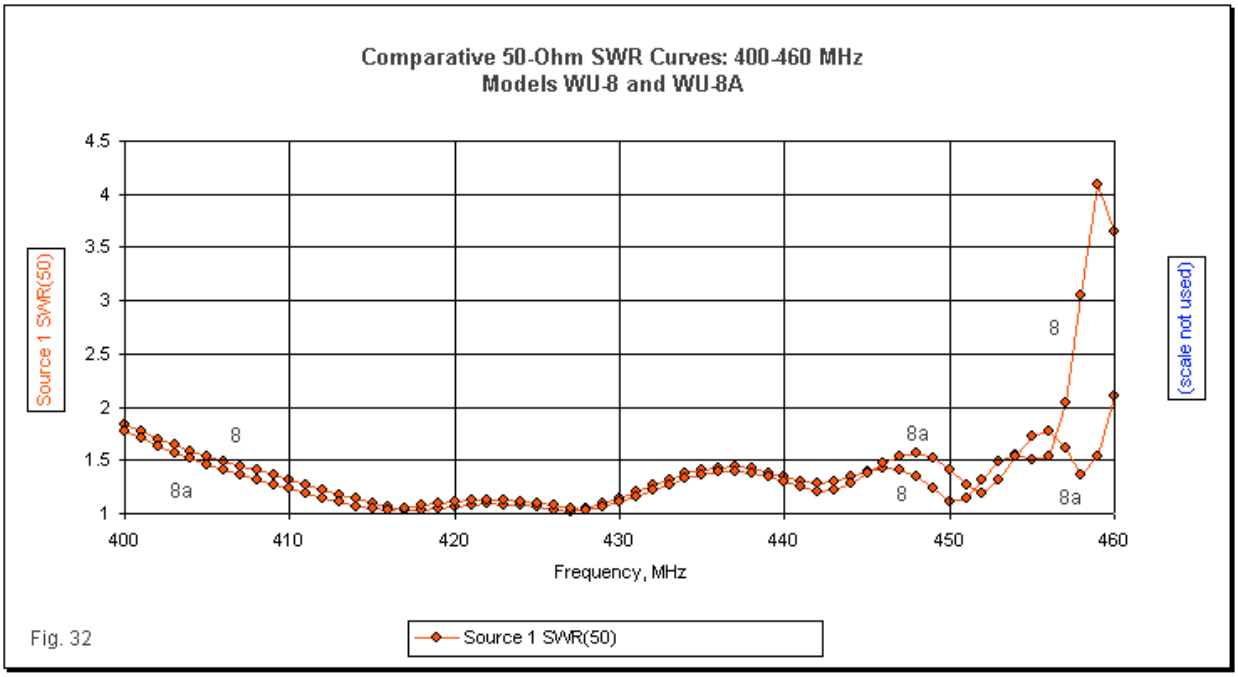

Fig. 32

From an operational perspective, all of the 20-element DL6WU Yagis will provide satisfactory performance within the 70-cm amateur band from 420 to 450 MHz. However, actual operation falls outside the purpose of this data accumulation. Its purpose is to provide data that may contribute to a better understanding of long-boom trimming Yagis, such as the DL6WU series.

It is likely that a more proper set of conclusions would have something of the following form.

1. To collect the most revealing data set on any given trimming Yagi involves looking at wide-band data covering virtually all of the operating passband for the array. Data taken only at or near the design frequency may obscure the behavior of the array and leave more mysteries than answered questions.

2. From a wide-band perspective--where wide-band may be defined relative to the operational passband for a given design--changes of element diameter and element spacing may make a considerable difference in the overall performance curve for an array at some given boomlength or number of elements. Hence, we cannot presume a carry-over of characteristics from one array version to the next. Undoubtedly, every set of trimming Yagis will show a set of front-to-back peak value and SWR dip lines. However, we cannot know how many and at what frequency without testing each variation we insert into a design.

3. The DL6WU and test Yagi series are both very wide-band designs as Yagis go, with very reasonable gain and usable front-to-back ratios across the region of workable 50-Ohm SWR values. The 70-cm band has a bandwidth of about 7% of the design frequency. The front-to-back and SWR cycles appear as a function of exerting less control over these operating parameters than over the basic feedpoint impedance and the forward gain. Other series of Yagis, whether or not they are true trimming arrays or simply arrays that may be extended with adjustments to one or more elements along the way, may exert design controls where the trimming Yagi sets do not. Hence, the existence of some cycles may not be universal to long-boom Yagi design.

4. The data suggest that some interactions among operating parameters may be considerably more complex than hitherto believed. For example, beamwidth is not a sole function of gain, but is also related to (at least) the front-to-sidelobe ratio. The strength of the forward sidelobes is to some degree related to the closeness of the frequency of maximum gain to the design frequency. Other designs may use the second and third directors--in addition to the impedance-setting cell--to provide additional control over the strength of sidelobes. Those controls may have an impact on the beamwidth of the array. As a second example, the cyclical nature of the feedpoint impedance data and the 180° front-to-back ratio suggest a relationship. However, that relationship is as yet undefined.

Indeed, this data accumulation is only that. It does not pretend to answer fundamental questions of Yagi design, but only to raise such questions and make such suggestions as the data themselves allow. Even then, the questions and suggestions are only those that occur at first sight. To see and formulate data patterns is not yet to offer an explanation.

Still, I have not seen anything like a complete data set for any long-boom trimming Yagi in the past. Although this accumulation is for 2 Yagi designs over one frequency range with one element diameter, I hope it is a step in the direction of having more complete data with which to work.

December 5, 2004